


Review

# Research Progress on the Application of One-Step Fabrication Techniques for Iridium-Based Thin Films in the Oxygen Evolution Reaction

Wenting Li <sup>1</sup>, Junyu Zhu <sup>1</sup>, Hongzhong Cai <sup>1,\*</sup> , Zhongqiu Tong <sup>2,\*</sup>, Xian Wang <sup>1</sup>, Yan Wei <sup>1</sup>, Xingqiang Wang <sup>1</sup>, Changyi Hu <sup>1</sup>, Xingdong Zhao <sup>1</sup> and Xuxiang Zhang <sup>1</sup>

- <sup>1</sup> Kunming Institute of Precious Metals, Kunming 650106, China; 17860365971@163.com (W.L.); zhujiy\_gys@163.com (J.Z.); wangxian@ipm.com.cn (X.W.); weiyang@ipm.com.cn (Y.W.); wxq@ipm.com.cn (X.W.); hcy@ipm.com.cn (C.H.); 19987870739@139.com (X.Z.); zxx@ipm.com.cn (X.Z.)
- <sup>2</sup> Faculty of Metallurgical and Energy Engineering, Kunming University of Science and Technology, Kunming 650093, China
- \* Correspondence: chz@ipm.com.cn (H.C.); zqtong@163.com (Z.T.)

**Abstract:** Electrochemical water splitting, a sustainable method for hydrogen production, faces the challenge of slow oxygen evolution reaction (OER) kinetics. Iridium oxide (IrO<sub>2</sub>) is widely regarded as the most effective catalyst for OER due to its excellent properties. Compared to nanoparticles, IrO<sub>2</sub> thin films exhibit significant advantages in OER, including a uniform and stable catalytic interface and excellent mechanical strength. This paper reviews recent advancements in one-step deposition techniques for the preparation of IrO<sub>2</sub> thin films and their application in OER. Additionally, it analyzes the advantages and disadvantages of various methods and the latest research achievements, and briefly outlines the future trends and applications.

**Keywords:** one-step deposition; IrO<sub>2</sub> thin films; OER; electrochemical deposition; physical vapor deposition; chemical vapor deposition



**Citation:** Li, W.; Zhu, J.; Cai, H.; Tong, Z.; Wang, X.; Wei, Y.; Wang, X.; Hu, C.; Zhao, X.; Zhang, X. Research Progress on the Application of One-Step Fabrication Techniques for Iridium-Based Thin Films in the Oxygen Evolution Reaction. *Coatings* **2024**, *14*, 1147. <https://doi.org/10.3390/coatings14091147>

Academic Editor: Alberto Palmero

Received: 10 August 2024

Revised: 28 August 2024

Accepted: 4 September 2024

Published: 6 September 2024



**Copyright:** © 2024 by the authors. Licensee MDPI, Basel, Switzerland. This article is an open access article distributed under the terms and conditions of the Creative Commons Attribution (CC BY) license (<https://creativecommons.org/licenses/by/4.0/>).

## 1. Introduction

In the past few decades, with societal development, the demand for energy has increased exponentially, necessitating a more intelligent and extensive approach to acquiring energy resources. Global warming and the depletion of fossil fuels have gradually raised awareness about the importance of developing new renewable energy sources, such as solar, wind, and hydro energy, which are key to sustaining development and minimizing negative environmental impacts [1–3]. Converting electrical energy into chemical energy in the form of fuels is an economically and environmentally sustainable solution for storing and transporting energy obtained from renewable energy systems [4–6]. Due to its high energy density and carbon-free nature, hydrogen energy is regarded as a promising method for hydrogen production through electrochemical water splitting [7,8]. Electrochemical water splitting refers to the process of decomposing water into hydrogen and oxygen through the hydrogen evolution reaction (HER) at the cathode and the OER at the anode [9,10], driven by electric power. However, the slow kinetics of the OER are the main factor limiting the efficiency of water electrolysis [11–13]. Platinum on carbon support (Pt/C) is commonly used for the HER cathode, while IrO<sub>2</sub>, known for its high conductivity, corrosion resistance, and stability, is currently the best catalyst for the OER anode [14–17].

In the water electrolysis catalytic process, the morphology and structural characteristics of the catalyst play a crucial role in determining its catalytic performance [18,19]. Although materials like IrO<sub>2</sub> nanoparticles theoretically exhibit excellent catalytic potential, their practical application is limited by several challenges, such as the tendency of particles to spontaneously aggregate, poor dispersion uniformity in the medium, and insufficient mechanical stability [20]. These bottlenecks directly lead to a significant reduction in the

effective active sites of the catalyst, thereby shortening its operational lifespan in real-world conditions and limiting its widespread application. In contrast, the application of IrO<sub>2</sub> catalysts in the form of thin films in water electrolysis technology highlights several significant advantages. Firstly, the thin-film structure creates a uniform and stable catalytic interface, fundamentally avoiding the common aggregation phenomena seen in nanoparticle or powder materials, thereby ensuring efficient catalytic reactions. Additionally, the dense structure and surface uniformity of the thin film not only enhance the catalyst's durability under high current density conditions but also ensure stability during long-term operation, effectively extending the overall lifespan of the catalyst [21]. Most critically, thin-film catalysts demonstrate excellent mechanical strength and superior substrate adhesion. This means that in the harsh environment of water electrolysis, the catalyst film can resist peeling or dissolution, maintaining the integrity and continuity of its structure and function. This characteristic is vital for ensuring the long-term stability and operational reliability of the catalyst and is a key factor in advancing water electrolysis technology towards greater efficiency and stability. With their unique structural advantages, IrO<sub>2</sub> thin-film catalysts provide a more reliable and efficient catalytic solution for the water electrolysis field.

Tables 1 and 2 present the performance data of iridium-based catalyst materials with different structures in the OER. We analyze these materials based on the following performance indicators: overpotential, iridium loading amount, Tafel slope, and stability test duration. According to the comparative analysis of the data from the tables, thin-film materials generally exhibit lower overpotentials, indicating that they can drive the reaction at lower voltages, thus demonstrating higher electrocatalytic efficiency. Although the Tafel slopes of thin-film and nanoparticle materials do not differ significantly, thin-film materials have notably lower iridium loading amounts. Moreover, in terms of stability, thin-film materials perform better; for instance, the stability test duration for p-L-IrO<sub>2</sub> reaches 2300 h [22]. Therefore, considering all performance indicators, iridium-based thin films demonstrate higher catalytic activity and long-term stability in the OER process, showing overall superiority over nanoparticle materials.

**Table 1.** OER performance parameters of Ir-based catalyst films reported in the literature.

Materials	Overpotential (mV)	Iridium Loading Amount (mg cm <sup>-2</sup> )	Tafel Slope (mV dec <sup>-1</sup> )	Stability Test Duration	Ref.
IrO <sub>2</sub> /Ti	-	0.100	53	-	[23]
IrTiO <sub>x</sub>	353	0.007	55	50 h	[24]
IrO <sub>2</sub> /NiO	285–316	0.160–0.270	45–60	-	[25]
IrO <sub>x</sub> /Ir/p <sup>+</sup> -n-Si	112	-	51–55	18 h	[26]
IrCrO <sub>x</sub> /FTO	430	-	59	-	[27]
Ir/Ti	330	-	30–40	20 h	[28]
IrO <sub>2</sub> /Ni	320	-	45	-	[29]
IrO <sub>2</sub> (100)/NiO	310–320	-	54–55	-	[30]
IrO <sub>x</sub> /TTLGDL	-	0.075–0.340	-	80 h	[31]
Au-Ir/CP	418–708	-	90–134	-	[32]
IrO <sub>2</sub> /Ti	-	0.4	-	300 h	[33]
α-IrO <sub>2</sub> /YSZ	300	-	250	-	[34]
IrHf <sub>x</sub> O <sub>y</sub>	370	-	50–66	6 h	[35]
p-L-IrO <sub>2</sub>	270	0.56	42.3	2300 h	[22]

**Table 2.** OER performance parameters of Ir-based catalyst nanoparticles reported in the literature.

Materials	Overpotential (mV)	Iridium Loading Amount (mg cm <sup>-2</sup> )	Tafel Slope (mV dec <sup>-1</sup> )	Stability Test Duration	Ref.
PbO <sub>2</sub> -IrO <sub>2</sub>	471	-	467	-	[36]
Pt/IrO <sub>2</sub> @MWCNT	270	-	85.1	-	[37]
Ti/SMST/IrO <sub>2</sub>	350	0.857	61	443 h	[38]
MW-IrO <sub>2</sub> /rGO	251	0.25	34.7	-	[39]
IrO <sub>2</sub> @TaO <sub>x</sub> @TaB	279	0.26	50	1500 h	[40]
Ir-IrO <sub>2</sub> /C-3	264	-	63.3	42 h	[41]
IrO <sub>2</sub> -BN-rGO	300	0.140	65.2	-	[42]
IrO <sub>2</sub> -c-BN	400	0.140	61.0	-	[42]
IrO <sub>2</sub> /TSO	263	0.131	51	200 h	[43]
IrO <sub>2</sub> @Co <sub>3</sub> O <sub>4</sub> -CoMoO <sub>4</sub>	236	-	46.5	6 h	[44]
IrO <sub>2</sub> /TNTs/Ti	400	0.514	-	550 h	[45]

One-step film formation refers to the process of directly forming a thin film through a single operational step, in which the primary composition and the main structure of the film are established in a single procedure. One-step film formation methods for preparing IrO<sub>2</sub> films include sol-gel methods [46,47], thermal decomposition [48], electrochemical oxidation [49], and sputtering [50,51]. Each method has its advantages and disadvantages. IrO<sub>2</sub> films prepared by the sol-gel method are fine and uniform with a high specific surface area, but the preparation process is complex, often requiring multiple coatings and heat treatments to form stable films. The thermal decomposition method is simple to operate with low raw material and equipment costs, but it requires high temperatures, resulting in high energy consumption, and it is difficult to control film uniformity and thickness, leading to unstable film performance. Electrochemical oxidation offers good controllability and high-purity products, but the reaction speed is slow, and although the equipment is relatively simple, achieving large-area uniform film formation remains challenging. Sputtering can directly deposit IrO<sub>2</sub> films on various substrates, achieving good control over film morphology and thickness. The IrO<sub>2</sub> films obtained by sputtering exhibit high activity and low overpotential, but the high equipment investment makes it unsuitable for large-scale batch production. Although chemical vapor deposition (CVD) and self-assembly methods are not as commonly used as other techniques for the preparation of IrO<sub>2</sub> thin films, primarily due to the complexity and high cost of CVD equipment and the reproducibility issues associated with self-assembly, each method has unique advantages. CVD allows for high coverage and region-selective deposition [52], while self-assembly enables precise structural control at the nanoscale, offering potential value for future research and innovation. Including these methods in a review provides a more comprehensive perspective, thereby fostering the development and application of new preparation techniques. Additionally, when IrO<sub>2</sub> catalysts are applied in the field of water electrolysis, coating techniques (such as spin coating and dip coating) are also commonly used strategies [53–55]. However, coated catalysts have several issues. The catalysts tend to aggregate or stack, leading to insufficient exposure of active sites and the formation of defect structures that are unfavorable for reactions. Moreover, the adhesion between the coated catalyst and the substrate is unstable, potentially leading to the catalyst detaching from the substrate surface under temperature changes, vibration, impact, or dynamic stress. The one-step film forming technology directly deposits IrO<sub>2</sub> film on the substrate surface to obtain a high-quality film structure and avoid the interface problems and defect accumulation caused by multiple film forming. This method not only simplifies the process and increases production efficiency but also significantly enhances the long-term stability and electrochemical performance of iridium-based film catalysts in OER by optimizing the uniformity and density of the films. Therefore, one-step film formation techniques show great potential and superiority in the application of IrO<sub>2</sub> film catalysts. They are expected

to play an important role in the energy conversion and hydrogen storage fields, driving further development of related technologies.

This paper comprehensively reviews the latest research developments in one-step fabrication techniques for iridium-based thin films in recent years, highlighting the crucial role of these films in enhancing OER catalytic performance. In light of the previous lack of systematic reviews focusing on the impact of one-step fabrication of IrO<sub>2</sub> thin films on OER catalytic efficiency, and considering the significant technical advancements in the preparation of various IrO<sub>2</sub> OER catalyst films in recent years, this paper aims to provide an extensive discussion. By deeply analyzing the meticulous design of material composition, innovative strategies for structural optimization, and specific measures for process improvement, this paper summarizes the latest research achievements in improving the OER performance of IrO<sub>2</sub> films. The goal is to offer valuable insights and references for researchers in related fields.

## 2. Catalytic Mechanism of Iridium Oxide in OER

Iridium oxide, as an efficient catalyst for the OER, has had its catalytic mechanism extensively and deeply explored and gradually clarified. Its excellent catalytic performance is primarily attributed to its unique electronic configuration and flexible multivalent state conversion characteristics [14,56–59].

In the OER process, the various oxidation states of iridium (such as Ir<sup>3+</sup>, Ir<sup>4+</sup>, and Ir<sup>5+</sup>) play a crucial role [14,58]. The transitions between these oxidation states not only help maintain charge balance within the reaction system but also facilitate the stable presence of reaction intermediates. Specifically, the transition of Ir<sup>4+</sup> to Ir<sup>5+</sup> during the catalytic process of IrO<sub>2</sub> significantly enhances its ability to adsorb and activate water molecules and reaction intermediates, effectively lowering the reaction energy barrier, thereby accelerating the formation of O-O bonds and the evolution of oxygen [58,60]. Simultaneously, the surface properties of IrO<sub>2</sub> are also critical to its catalytic performance. Its surface can robustly adsorb key intermediates such as OH<sup>−</sup> and O<sup>2−</sup>, and through finely tuned electron and proton transfer processes, it promotes the efficient formation of O-O bonds. In this process, the active oxygen species formed on the IrO<sub>x</sub> surface play a central role. These species react with water molecules to form O-OH intermediates, ultimately leading to the release of oxygen. The stable capture and efficient conversion of these intermediates are key to the high catalytic activity of IrO<sub>2</sub>. Furthermore, the catalytic cycle efficiency of IrO<sub>2</sub> is a testament to its outstanding performance. Its OER catalytic cycle encompasses multiple pathways, involving the redox cycles of the Ir center, the conversion of surface adsorbed oxygen species, and the participation of lattice oxygen in complex processes. Among these, the pathway centered on the Ir<sup>5+</sup> intermediate is particularly critical. In this pathway, Ir<sup>5+</sup> reacts with water or OH<sup>−</sup> to form peroxide species (OOH), ultimately achieving efficient oxygen release. This multi-pathway cycle mechanism ensures the high efficiency of IrO<sub>2</sub> catalysts in the OER.

In the study of the OER mechanism, the Adsorbate Evolution Mechanism (AEM) and the Lattice Oxygen Mechanism (LOM) are the two main theories, as illustrated in Figure 1 [61,62]. Although the traditional AEM is constrained by the linear relationship of intermediate adsorption energies, facing a limit on the minimum overpotential, the LOM theoretically further reduces the OER overpotential by involving lattice oxygen. However, LOM still encounters thermodynamic challenges in practical applications, such as the slow deprotonation steps and catalyst stability issues due to lattice oxygen release. To address these problems, a novel theory called the lattice water-assisted oxygen exchange mechanism has been proposed [63,64]. This mechanism accelerates the OER process and enhances catalyst stability through the direct involvement of lattice water molecules. During the reaction, lattice water molecules near the active sites can quickly transfer and dissociate into \*OH intermediates, facilitating subsequent oxygen exchange. This dynamic process not only accelerates the oxygen generation rate but also maintains the structural stability of the catalyst through the rapid replenishment and redissociation of external water molecules.

As a result,  $\text{IrO}_x \cdot n\text{H}_2\text{O}$  demonstrates higher intrinsic activity and excellent electrochemical stability in the OER.

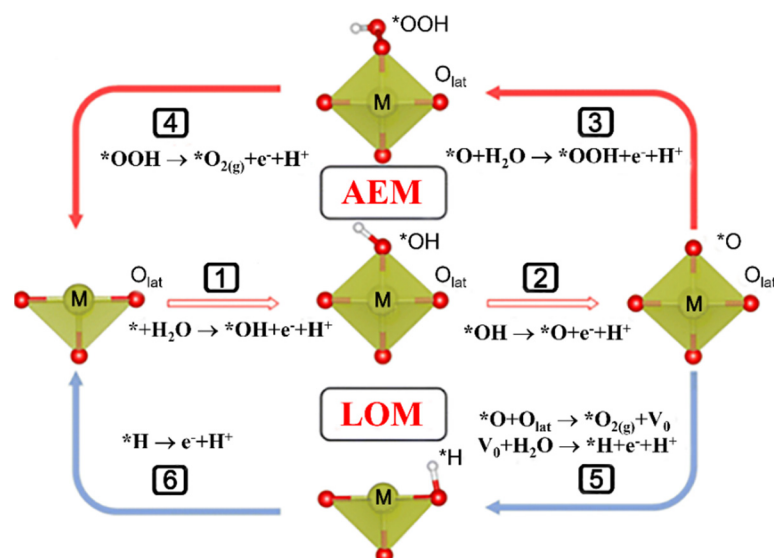


**Figure 1.** The two main theories in the study of the OER mechanism: the Adsorbate Evolution Mechanism (AEM) and the Lattice Oxygen Mechanism (LOM) [61].

### 3. One-Step Fabrication Techniques for Iridium-Based Thin Films

In the preparation of iridium-based thin films for application in the OER, techniques such as electrochemical deposition, physical vapor deposition, chemical vapor deposition, and sol-gel methods have demonstrated exceptional technical advantages. These methods enable the successful one-step fabrication of thin films, effectively avoiding the defects and interface issues that may arise from traditional multi-step processes, thereby significantly enhancing the performance of  $\text{IrO}_2$  films. Through the application of these advanced techniques, iridium-based thin films have exhibited superior catalytic activity and long-term stability in OER, injecting new vitality into the development of fields such as water electrolysis for hydrogen production and fuel cells.

#### 3.1. Electrochemical Deposition Method

Electrochemical deposition is a method that utilizes electrochemical reactions to deposit the desired material on the surface of an electrode [65]. In the preparation of  $\text{IrO}_2$  thin films, the process generally consists of the following steps. Initially, an electrolyte solution containing iridium salts is prepared, and the working and reference electrodes are placed into the electrochemical cell. Electrochemical deposition is then carried out by controlling the current or voltage, which allows iridium ions to deposit onto the electrode surface and form the thin film. Once deposition is complete, the electrode is removed from the electrolyte solution and cleaned with an appropriate solvent to eliminate any residual electrolyte. Finally, heat treatment or other post-processing techniques are applied to improve the film's structure and properties. By precisely controlling electroplating parameters—such as current density, deposition time, and electrolyte concentration—the deposition rate and film thickness can be accurately managed, resulting in continuous, uniform, and strongly adherent  $\text{IrO}_2$  films directly on the substrate in a single operation. Due to its advantages of mild preparation conditions, high degree of mechanization, and simple operation, electrochemical deposition is highly suitable for preparing  $\text{IrO}_2$  film electrodes for the OER. Based on the technique of electric field generation, several common electroplating methods include constant current deposition, constant voltage deposition, pulse deposition, cyclic voltammetry deposition, and assisted field deposition.

Electrodeposition usually occurs under mild conditions (room temperature and atmospheric pressure), avoiding damage to the substrate material that high temperature and high pressure can cause. This makes electrodeposition advantageous for substrate selection, as it is suitable for a broader range of materials, including metals, carbon-based materials, and porous materials, meeting diverse application needs and providing greater flexibility in process design and optimization. Common substrate materials for electrodepositing IrO<sub>2</sub> layers include Pt, Au, Ti, glassy carbon (GC), carbon paper (CP), and stainless steel [33,66–70]. The electrochemical behavior and stability of electrodeposited IrO<sub>2</sub> vary with different substrates. Lee et al. [67] electrodeposited a thin layer of IrO<sub>x</sub> on carbon-based CP and studied its OER performance in proton exchange membrane water electrolysis (PEMWE). Using a Nafion 212 membrane (operating at 90 °C), they achieved a high water splitting current density of 1.92 A/cm<sup>2</sup> at 1.8 V with a low iridium loading of 0.1 mg<sub>Ir</sub>/cm<sup>2</sup>. However, using carbon paper as the anode PTL resulted in lower PEMWE stability due to carbon corrosion caused by carbon oxidation. To address this issue, Choe et al. [33] replaced the CP with a porous titanium substrate, electrodeposited an IrO<sub>x</sub> layer onto the Ti porous transport layer (Ti PTL), and compared it with iridium oxide produced by sputtering. The results showed (Figure 2a) that the IrO<sub>x</sub> film on the titanium mesh exhibited excellent electrochemical performance, particularly in stability and durability under high-temperature and high-current-density conditions, far superior to sputtering and electrodeposited films on CP. Additionally, the IrO<sub>x</sub> layer served not only as a catalyst but also as a corrosion-resistant layer for the Ti PTL (Figure 2b). The PEMWE prepared with the IrO<sub>x</sub>-coated Ti PTL and Nafion 212 membrane achieved a current density of 0.97 A/cm<sup>2</sup> at 1.6 V and 120 °C with a low iridium loading of 0.4 mg<sub>Ir</sub>/cm<sup>2</sup>. Wu et al. [66] studied the anodic electrodeposition process of IrO<sub>x</sub> on different substrates. The study found that the electrocrystallization process of IrO<sub>x</sub> exhibited a diffusion-controlled three-dimensional nucleation process on different substrates, and a nucleation model was established to describe this process. According to the nucleation model parameters, iridium oxide showed excellent nucleation performance on titanium substrates, which had the highest nucleation rate and active nucleation sites. As shown in Figure 2c,d, the overpotential and Tafel slope for IrO<sub>x</sub> deposited on Au substrates were the lowest compared to other substrates. The  $k_{OER}$  value, indicating the oxygen evolution rate constant, was the highest for IrO<sub>x</sub> electrodeposited on gold substrates, suggesting that IrO<sub>x</sub> deposited on gold supports more favorable OER kinetics. This is consistent with the previous study by Abyaneh et al. [71], which indicated that the secondary redox process affects the changes in potentiostatic current transients and that growth is limited by the binding rate of adatoms to three-dimensional (3D) growth centers.

During the electrochemical deposition process of IrO<sub>2</sub> catalysts, the content of internal oxygen elements significantly and profoundly impacts the electrochemical performance of the catalysts ultimately deposited on the substrates [72,73]. This is dependent on the interaction between the catalyst and the substrate and can serve as a descriptor of OER activity. Cho et al. [70] synthesized efficient amorphous IrO<sub>x</sub> on Ti substrates (TS) using an electrodeposition process and observed the relationship between the electronic structure and electrochemical performance of electrodeposited IrO<sub>x</sub> during the OER in PEMWE. Through a combined analysis of experiments and first-principles calculations, it was found that an electronic interaction occurs between the electrocatalyst and the substrate. The interaction between IrO<sub>x</sub> and the Ti substrate induced the migration of oxygen sources from the oxide to the metal, resulting in electrophilic activation of the oxygen sites that were depleted of oxygen in the IrO<sub>x</sub>. These activated oxygen sites exhibited lower activation energy for water adsorption, which is one of the reasons for their high OER activity. As shown in Figure 3, the interaction between Ir and O atoms distorted the ordered structure of IrO<sub>2</sub>, forming mesoporous structures. The electrophilic oxygen defects and mesoporous Ir oxide structure led to high intrinsic OER activity. Building on this, Oyshi et al. [74] electrodeposited Au and IrO<sub>x</sub> on TS and found that the transferred oxygen oxidized the substrate, forming TiO<sub>2</sub>, which had a synergistic effect with the electronic state of Au.

This synergy facilitated the transfer of reaction molecules to the catalytic surface, and the presence of Ir supported redox reactions, enhancing the overall electrochemical conversion kinetics of the reaction system. Electrochemical parameters such as turnover frequency (TOF), Tafel slope, and exchange current density ( $j_k$ ) were superior to those of electrodes used in other experiments.

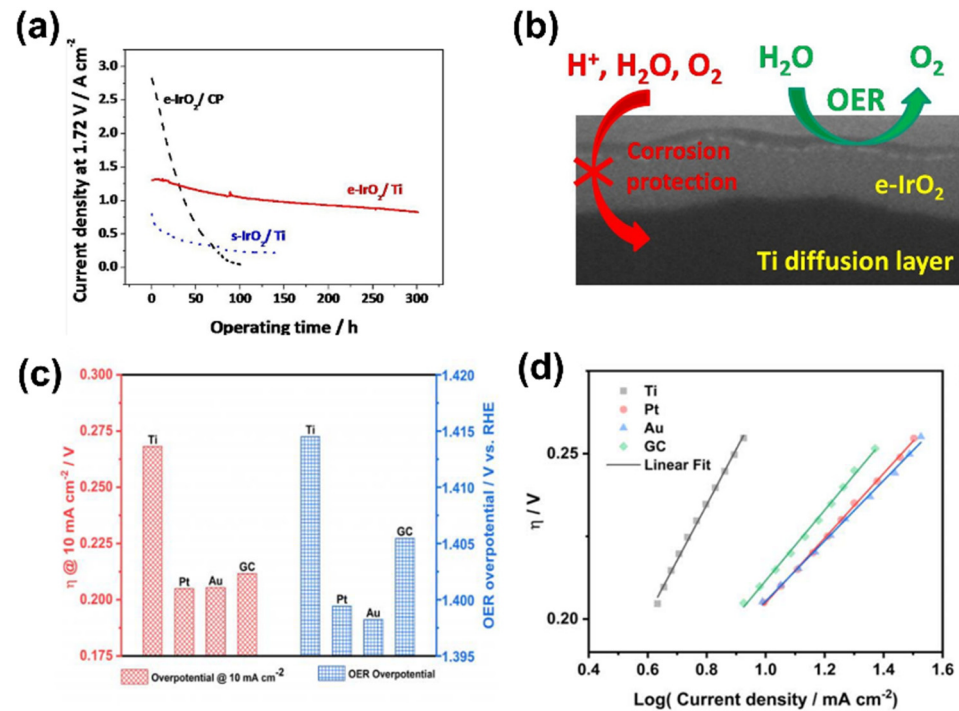


**Figure 2.** (a) Variation of the current density of IrO<sub>2</sub> films electrodeposited on carbon paper (e-IrO<sub>2</sub>/CP) and titanium mesh (e-IrO<sub>2</sub>/Ti) and IrO<sub>2</sub> films sputtered on titanium mesh (s-IrO<sub>2</sub>/Ti) at a potential of 1.72 V/A cm<sup>−2</sup> over time [33]. (b) Mechanism of action of IrO<sub>2</sub> thin films electrodeposited on titanium mesh (e-IrO<sub>2</sub>/Ti) in OER [33]. (c) Overpotential of IrO<sub>x</sub> deposited on different substrates (Ti, Pt, Au, Gc) @ 10 mA cm<sup>−2</sup> and OER overpotential. (d) Tafel slope of IrO<sub>x</sub> on different substrates (Ti, Pt, Au, Gc) [66].

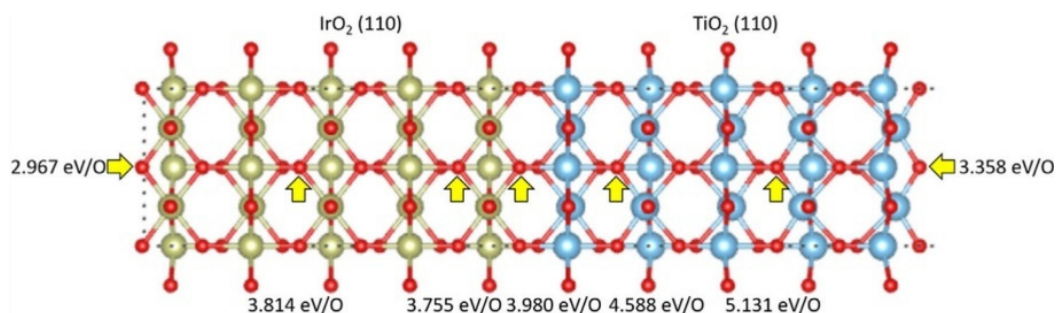


**Figure 3.** DFT-based calculation of the difference in the oxygen vacancy formation energy to extract a single oxygen atom at various locations in IrO<sub>2</sub> || TiO<sub>2</sub> [70].

Electrochemical deposition is a low-cost, environmentally friendly, and easily scalable method for preparing iridium oxide electrodes, and it is relatively mature in current research [75–77]. In the latest studies, Lei Ding and his team [31] prepared amorphous IrO<sub>x</sub> thin film electrodes via electrodeposition, achieving a catalyst loading of only 0.075 mg/cm<sup>2</sup>, which is significantly more efficient compared to the 2 mg/cm<sup>2</sup> loading of commercial catalyst coatings. This method not only saves over 96% of the catalyst but also increases utilization by 42 times. This groundbreaking advancement highlights the unique

advantages of electrochemical deposition in precisely controlling the one-step fabrication of iridium oxide thin films and indicates its vast potential applications in iridium oxide electrodes and broader electrochemical catalysis fields. As researchers continue to explore and optimize electrochemical deposition technology, we have reason to believe that this technique will play an increasingly important role in key renewable energy technologies such as water electrolysis for hydrogen production and fuel cells. It will provide robust technical support for achieving global green energy transitions and sustainable development goals.

### 3.2. Physical Vapor Deposition Method

Among the numerous preparation methods, physical vapor deposition (PVD) has garnered significant attention due to its unique advantages. The PVD method for preparing iridium oxide films for OER offers benefits such as high purity, excellent film adhesion, and good uniformity [78–80]. However, its complex equipment, high costs, and limitations in large-area preparation are factors that need consideration. PVD encompasses various methods, mainly including sputter deposition [81], electron beam evaporation [82], and pulsed laser deposition [30,83,84]. Sputtering provides good film uniformity and high density but is energy-intensive; electron beam evaporation can achieve high-purity films but may result in films with many pores and defects; pulsed laser deposition is favored for its precise control and high-quality films but involves expensive and complex equipment.

Sputtering technology is an advanced physical vapor deposition method that utilizes high-energy particles (such as argon ions,  $\text{Ar}^+$ ) to bombard the surface of the target material, causing the target atoms or molecules to detach and deposit onto the substrate to form a thin film. Depending on the process and equipment, sputtering can be classified into reactive sputtering [85,86], magnetron sputtering [87], radio frequency sputtering [88,89], and direct current sputtering [90,91], among others. One-step film formation using the sputtering method to prepare  $\text{IrO}_2$  films shows great potential in OER applications. By precisely controlling the target composition and sputtering conditions, it is possible to produce high-purity, compositionally uniform  $\text{IrO}_2$  films in one step, effectively avoiding subsequent complex processing steps and potential contamination issues. Due to the high density and uniformity of the films, iridium oxide films prepared by sputtering exhibit excellent electrochemical performance. The process parameters for preparing  $\text{IrO}_2$  films include target power, voltage, substrate temperature, and the flow ratio of oxygen to argon gases. By controlling these process parameters, the surface morphology of the films can be adjusted to expose more active sites, thereby enhancing the catalytic performance of the OER [92,93]. Slavcheva et al. [94] studied the use of reactive magnetron sputtering to deposit  $\text{IrO}_2$  films as water electrolysis catalysts in polymer electrolyte membrane (PEM) cells. They investigated the mechanical stability, corrosion resistance, and catalytic activity of  $\text{IrO}_2$  films with different sputtering thicknesses and loadings under high anode potentials. The study found that when the  $\text{IrO}_2$  film thickness was 500 nm and the loading was  $0.2 \text{ mg/cm}^2$ , the anode current density reached  $0.3 \text{ A/cm}^2$  at a potential of 1.55 V (versus RHE), demonstrating optimal OER performance. Figure 4a shows the anode steady-state polarization curves of sputtered  $\text{IrO}_2$  films (SIROFs) of different thicknesses at  $80^\circ\text{C}$ , with the 500 nm thick SIROFs exhibiting the lowest overpotential and the best catalytic activity for the OER. Subsequently, Tachikawa et al. [23] examined the effect of annealing temperature on the OER activity of  $\text{IrO}_2$  films prepared by sputtering in  $0.5 \text{ M H}_2\text{SO}_4$  solution. As depicted in Figure 4b–d, it can be observed that the OER active area decreases with the increase in annealing temperature. This phenomenon can be attributed to the reduction in electrochemical double-layer capacitance (EDLC), indicating a lower density of active sites. Furthermore, higher annealing temperatures lead to an increase in the crystallinity of the thin film.



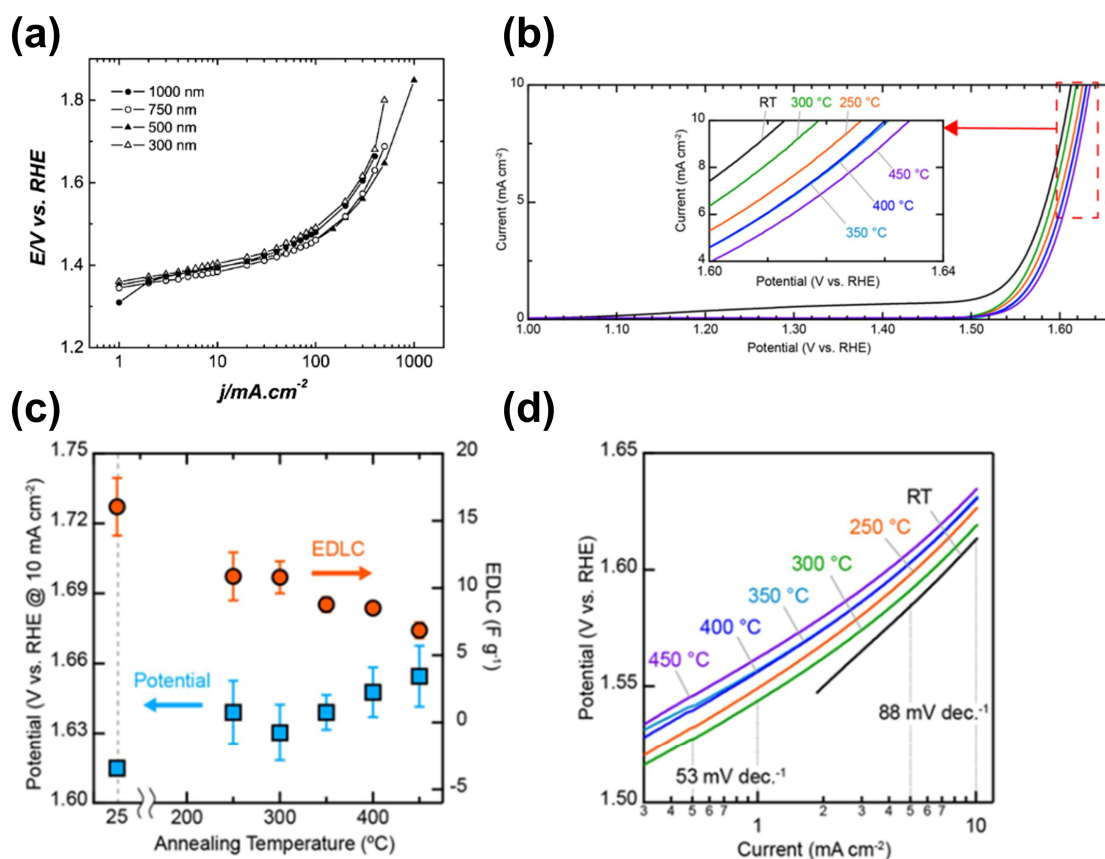


**Figure 4.** (a) Dependence of current density  $j_a$  at 1.31 V on the scan rate for catalytic films with different thickness; test temperature 20 °C [94]. (b) First-cycle LSV curves of sputtered IrO<sub>2</sub> films at different annealing temperatures; (c) Relationship between annealing temperature, potential at 10 mA cm<sup>-2</sup>, and EDLC. (d) Tafel plots of IrO<sub>2</sub> films [23].

Electron beam physical vapor deposition (EBPVD) utilizes an electron beam to heat and evaporate the target material, causing the vapor to deposit on the substrate and form a thin film [95]. The process of EBPVD involves several key steps: initially, an electron beam is used to heat and evaporate the target material, converting it into a vapor of atoms or molecules; subsequently, these vapors diffuse in a vacuum environment and reach the substrate surface; then, the evaporated atoms or molecules condense on the substrate, gradually forming a thin film; finally, the thickness and uniformity of the film can be precisely controlled by adjusting deposition parameters such as electron beam power, substrate temperature, and deposition time. Compared to sputtering, iridium-based films prepared by EBPVD may have more pores and defects, resulting in lower film density and uniformity, fewer surface active sites, and compromised mechanical properties, making the films more prone to dissolution and deactivation during electrochemical reactions. Geiger et al. [82] used the electron beam evaporation method to prepare iridium thin-film electrodes and formed hydrated IrO<sub>2</sub> film electrodes through electrochemical methods. Both sets of electrodes underwent heat treatment, and their activity and stability in the OER were studied. However, as evident from Figure 5a, the iridium films obtained through sputter deposition exhibit superior electrochemical performance, particularly when subjected to heat treatment at 400 °C and 500 °C.

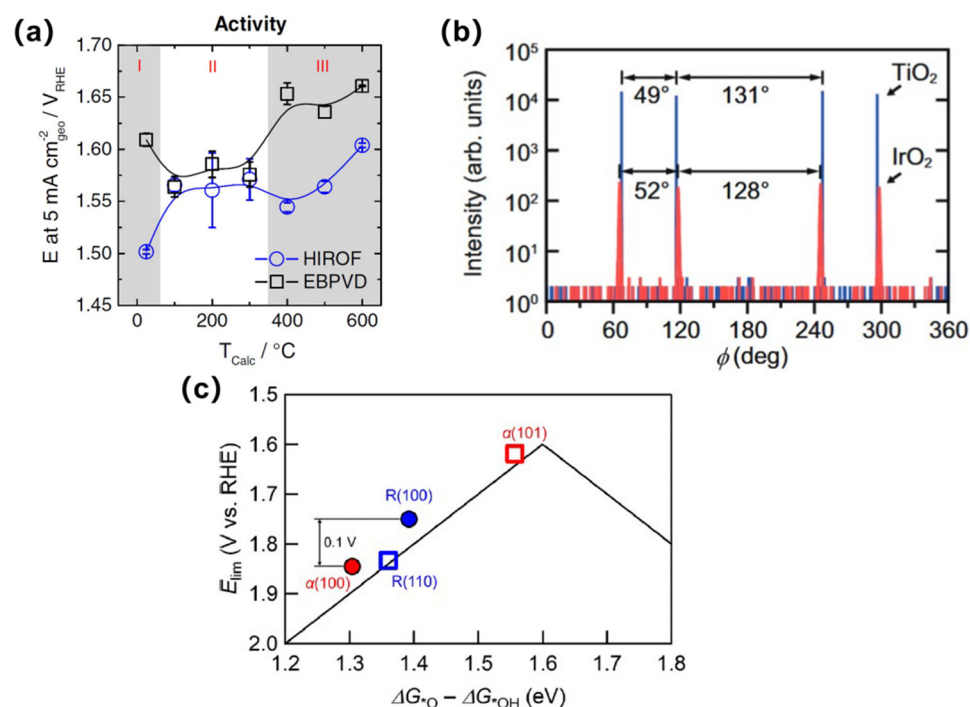


**Figure 5.** (a) The effect of annealing temperature on activity of the as-prepared iridium film (EBPVD) and the hydrous iridium oxide film (HIROF) measured with a linear sweep of potential ( $10 \text{ mV s}^{-1}$ ) from 1.2 V RHE to a potential corresponding to the current density of  $5 \text{ mA cm}^{-2}_{\text{geo}}$  [82]. (b) XRD  $\Phi$ -scans for a 60 nm thick IrO<sub>2</sub> film and the TiO<sub>2</sub> substrate (101) peaks. (c) Theoretical OER activity volcano plot of the studied columbite and rutile IrO<sub>2</sub> surfaces constructed from universal scaling.  $\alpha$  (hkl) and R(hkl) refer to the (hkl) surface of columbite and rutile IrO<sub>2</sub>, respectively [34].

Pulsed laser deposition (PLD) employs high-energy pulsed laser irradiation on a target material, causing its surface to instantly vaporize and generate a plasma plume. Subsequently, this plasma expands within a vacuum or low-pressure environment and reaches the substrate surface; finally, the atoms or ions within the plasma condense onto the substrate, gradually forming a thin film. The PLD method allows for precise control of the film, producing IrO<sub>2</sub> films with excellent crystal quality and surface smoothness. This method is suitable for preparing multilayer films and heterostructure films [96], enabling good interface bonding between different materials. However, PLD equipment is expensive, the operation is complex, and it is not suitable for large-area industrial production of thin films. PLD technology is commonly used for depositing iridium films on precision devices such as semiconductor devices, and more research and development are needed for its application in preparing IrO<sub>2</sub> films for OER electrode catalyst layers. Hou et al. [97] used PLD to prepare IrO<sub>2</sub> films on TiO<sub>2</sub> substrates at 500 °C and 100 mTorr O<sub>2</sub> pressure. The study found that grain boundaries limited the conductivity of the films at low temperatures, and strain relaxation seemed to cause stacking faults at the grain boundaries. Therefore, finely tuning the grain boundary structure of IrO<sub>2</sub> films and effectively reducing internal defects are key steps to significantly enhancing the catalytic performance of this material in OER. Additionally, binary IrO<sub>2</sub> with non-rutile structures have also shown potential as efficient and stable OER catalysts, making them promising candidates. In recent research, Lee et al. [34] used PLD to grow epitaxial films of ilmenite-type IrO<sub>2</sub>. As depicted in Figure 5b,c, the thin film can be optimized to achieve a preferred (100) orientation of  $\alpha$ -IrO<sub>2</sub>, exhibiting a lower overpotential in the oxygen evolution reaction (OER) compared to rutile IrO<sub>2</sub> (100).

Using the PVD method for one-step fabrication of IrO<sub>2</sub> films offers multiple advantages when the films are used as OER catalysts. The films grown by PVD have high purity, effectively eliminating contaminants such as sulfur, chlorine, and other unwanted

elements or compounds commonly found in precursors used in wet chemical methods. These contaminants can often reduce the catalyst's activity and stability. Additionally, PVD technology offers strong controllability and high production efficiency during the preparation process, making it favorable for the large-scale production of IrO<sub>2</sub> film catalysts. With continuous advancements in PVD technology, the preparation of IrO<sub>2</sub> film catalysts will become more refined and scalable, promising to play an even greater role in the field of water electrolysis.

### 3.3. Chemical Vapor Deposition Method

Chemical vapor deposition (CVD) is a technique in which precursors undergo chemical reactions on the substrate surface at high temperatures to form thin films [98,99]. CVD technology achieves one-step film formation by introducing precursor gases into a heated reaction chamber, where they undergo chemical reactions under high temperatures or other energy sources, generating and depositing the target material as a thin film while removing byproducts. The process concludes with cooling and any necessary post-treatment to enhance the film's properties. Common CVD techniques include metal-organic chemical vapor deposition (MOCVD) [100–102] and plasma-enhanced chemical vapor deposition (PECVD) [103]. MOCVD uses metal-organic compounds as precursors, forming thin films on the substrate surface through thermal decomposition reactions. It is suitable for high-temperature deposition and can produce high-purity films. PECVD, on the other hand, introduces plasma into the CVD process, providing additional energy to reduce deposition temperature, increase deposition rate, and improve film quality.

In the CVD process, the choice of precursor is crucial because it directly affects the formation, characteristics, and functionality of the film. The precursor needs to have an appropriate vapor pressure and a sufficient temperature window to ensure that it does not decompose prematurely during transport and effectively decomposes on the substrate surface [104]. PECVD precursors need to remain stable under low-temperature and plasma conditions while being able to decompose effectively. Commonly used gaseous or low-boiling-point liquid precursors include iridium tetrafluoride (IrF<sub>4</sub>), bis(1,5-cyclooctadiene)iridium (Ir(COD)<sub>2</sub>), methylcyclopentadienyl iridium (Ir(MeCp)<sub>2</sub>), and ethylcyclopentadienyl(1,5-cyclooctadiene)iridium (Ir(EtCp)(1,5-COD)) [105–107]. In contrast, MOCVD precursors need to exhibit good volatility and thermal stability at high temperatures. Commonly used liquid or solid organometallic compounds include Ir(acac)<sub>3</sub> (iridium acetylacetonate) and Ir(thd)<sub>3</sub> (iridium 2,2,6,6-tetramethyl-3,5-heptanedionate). Precursors need to decompose at high temperatures to form metal or metal oxide films, such as Ir(COD)(MeCp) (methylcyclopentadienyl 1,5-cyclooctadiene iridium), which is used for iridium film deposition at 573–673 K. Early Ir precursors such as IrCl<sub>3</sub>, IrCl<sub>4</sub>, and IrBr<sub>3</sub> tended to introduce impurities, affecting film performance. The new generation of Ir precursors includes Ir (I) and Ir (III) compounds, and by adjusting neutral ligands and anionic ligands, their volatility, thermal stability, and reactivity can be precisely tuned to promote the reaction process. The main differences between PECVD and MOCVD precursors lie in their stability, reactivity, and decomposition temperatures. These differences directly impact the application range and quality of the films produced by the two processes.

Maury et al. [108] used Ir(COD)(MeCp) as a precursor to grow iridium coatings at low temperatures ranging from 573 K to 673 K in a hot-wall CVD reactor through MOCVD technology. The study found that in the presence of oxygen, the iridium coatings exhibited higher purity and growth rates. However, high concentrations of oxygen led to the co-deposition of Ir and IrO<sub>2</sub>. Using oxygen as a co-reagent prevented carbon incorporation and significantly increased the growth rate (Figure 6a). Hernández et al. [109] used Ir(acac)<sub>3</sub> as a precursor to develop phase diagrams for the formation of iridium and IrO<sub>2</sub> films using CVD technology. They studied the formation regions under different temperature and oxygen partial pressure conditions. Figure 6b shows that metallic iridium primarily formed at lower oxygen partial pressures (<2 Pa), while iridium oxide was more likely to form at higher oxygen partial pressures (>2 Pa) and higher temperatures (500–600 °C). The optimal

deposition conditions were moderate temperatures and oxygen partial pressure to achieve high-quality iridium film deposition. Building on this, Yan et al. [110] introduced a new solid precursor,  $\text{Ir}(\text{thd})_3$  (thd = 2,2,6,6-tetramethyl-3,5-heptanedione), for MOCVD preparation of iridium films. The experiments showed that this precursor had higher volatility than  $\text{Ir}(\text{acac})_3$  and successfully synthesized iridium films on glass substrates at 400 °C. As shown in Figure 6c, the films exhibited an island-like structure, following the Volmer–Weber growth mode. Jürgensen et al. [105] studied a method for preparing nanostructured  $\text{IrO}_x$  films using PECVD technology. They successfully deposited amorphous  $\text{IrO}_x$  films on substrates such as silicon, alumina, FTO, and gold by decomposing a novel heteroleptic Ir(I) precursor [ $(\text{CO})_2\text{Ir}(\text{TFB-TFEA})$ ]. These films were converted into highly catalytically active  $\text{IrO}_2$  films during subsequent annealing, demonstrating excellent electrochemical performance. As illustrated in Figure 7a,b, it is evident that the  $\text{IrO}_x/\text{Au}/\text{Cu}$  film exhibited a highly efficient OER activity with an overpotential of approximately 0.35–0.60 V at a current density of 10 mA/cm<sup>2</sup> in 1 M KOH electrolyte.

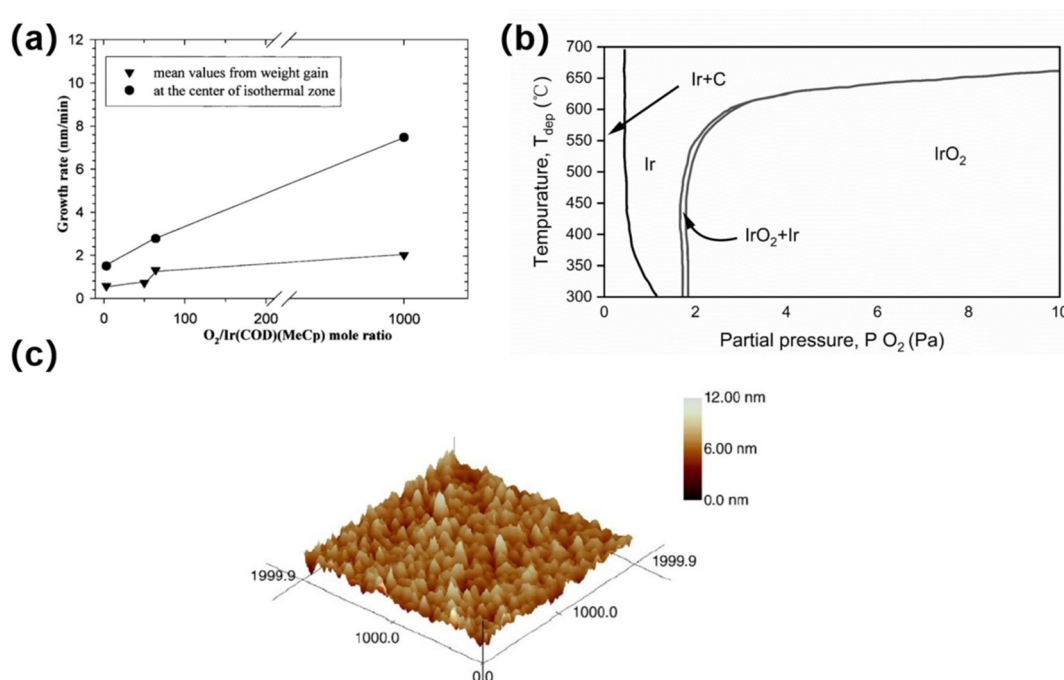


**Figure 6.** (a) Influence of the reactive gas phase composition on the growth rate of Ir coating deposited at 573 K [108]. (b) Calculation of the Ir-CVD phase diagram for the iridium  $\text{Ir}(\text{acac})_3$ - $\text{O}_2$ -Ar gas mixture as a function of  $\text{O}_2$  partial pressure and deposition temperature [109]. (c) The AFM stereo images of the iridium films [110].

In CVD, besides MOCVD and PECVD, there are several other methods, such as low-pressure chemical vapor deposition (LPCVD) [111–113], high-density plasma chemical vapor deposition (HDPCVD) [114,115], hot-wire chemical vapor deposition (HWCVD) [116,117], direct liquid injection chemical vapor deposition (DLI-CVD) [118,119], photo-chemical vapor deposition (Photo-CVD) [120], and electrochemical vapor deposition (ECVD) [121]. Each method has its unique advantages and specific applicability, which meet the needs of different materials and applications. However, their use in the preparation of  $\text{IrO}_2$  films is limited, and due to insufficient research in this area, they are not discussed in detail here. To understand the reasons for their limited application in  $\text{IrO}_2$  film deposition and their impact on oxygen evolution reaction (OER) performance, the specific limitations of each method are outlined below: LPCVD, while capable of enhancing film uniformity, requires high deposition temperatures, which may lead to phase transitions or structural defects within the films, thereby affecting the catalytic activity and stability in OER; HDPCVD utilizes high-density plasma, which could introduce impurities or result in non-uniform microstructures, diminishing its

electrocatalytic performance in OER; HWCVD relies on high-temperature metal filaments to decompose precursors, making it challenging to achieve uniform film deposition and potentially causing uneven electrode surfaces that negatively impact OER activity; DLI-CVD requires precise control over the injection and vaporization of liquid precursors, making the process complex and costly; Photo-CVD relies on a light source to initiate reactions, often resulting in poor film uniformity and potentially leading to non-uniform OER activity regions; moreover, ECVD has a relatively low deposition rate, and its application in IrO<sub>2</sub> film deposition is not well-studied, which limits its potential as an effective OER catalyst. These limitations restrict the broader application of these methods in the preparation of high-quality IrO<sub>2</sub> films and the enhancement of OER performance.

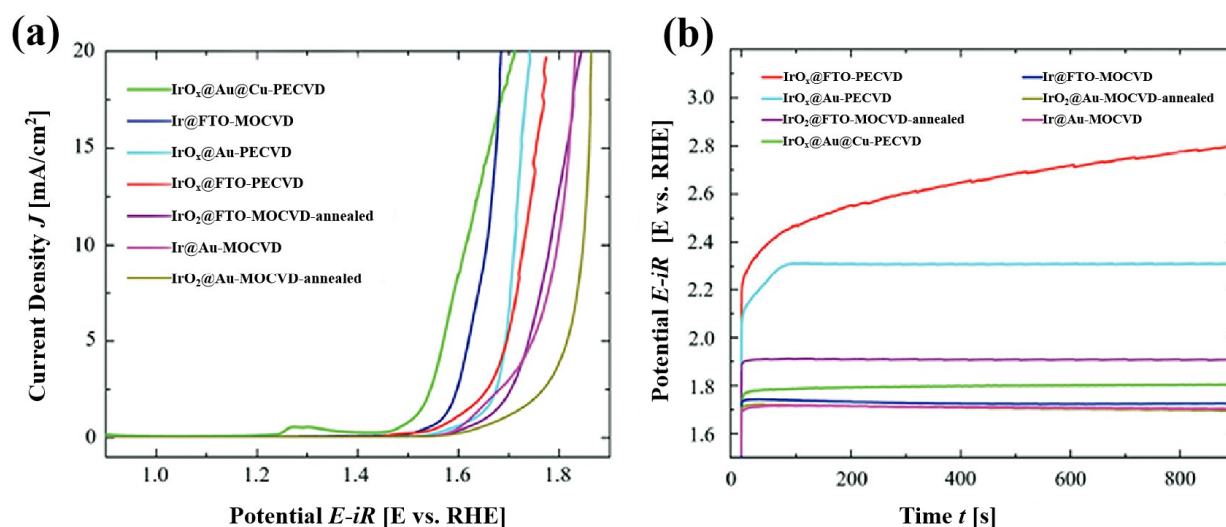


**Figure 7.** (a) Current densities  $J$  of different prepared electrodes against applied potential  $E$ . (b) Time-dependent potentials  $E$  of iridium-based substrates at different deposition condition at 10 mA/cm<sup>2</sup> (1 M KOH) [105].

### 3.4. Sol–Gel Method

The sol–gel method is a technique for preparing inorganic thin films or nanomaterials by dissolving precursors to form a sol, followed by gelation, drying, and heat treatment. Through solution processing and simple deposition techniques, the sol–gel method allows for the one-step fabrication of uniform and high-quality IrO<sub>2</sub> films on substrate surfaces, showing potential for application in OER catalysis.

The sol–gel method is one of the simplest chemical methods for film preparation. Sol–gel deposition typically requires heat treatment at 300 °C to successfully form IrO<sub>2</sub> from its precursor state. Suitable iridium salts, such as IrCl<sub>3</sub> or iridium acetate precursors, are selected and dissolved in an appropriate solvent, then chelating agents and polyols are added to form a sol. The sol is then applied to the substrate using spin-coating or dip-coating methods. After drying and high-temperature treatment, IrO<sub>2</sub> nanoparticle films can be obtained [46,122]. The sol–gel method allows for the one-step preparation of IrO<sub>2</sub> films on electrodes. The film thickness can be initially controlled by adjusting the sol concentration and the number of coatings, but there may still be some issues with thickness uniformity. High-temperature treatment is necessary to obtain crystalline IrO<sub>2</sub> films, but it may damage the electrode material. Common sol–gel routes include the Pechini method [123], traditional sol–gel method, alkoxide hydrolysis method [124,125], inorganic–organic hybrid method [126], and supercritical sol–gel method [127], among others. Guan et al. [128] described a technique for preparing amorphous IrO<sub>x</sub> films by spin-casting H<sub>2</sub>IrCl<sub>6</sub>/polyvinylpyrrolidone (PVP) on FTO substrates (Figure 8a), followed by annealing at 300 °C and air plasma treatment. In 0.5 M H<sub>2</sub>SO<sub>4</sub> electrolyte, these films exhibited excellent catalytic performance for the OER process at room temperature (RT),

with an overpotential of 0.291 V @ 10 mA/cm<sup>2</sup>, a Tafel slope of 0.0554 V/dec, and an ultra-high mass activity of 993 A/g at 1.55 V. In recent studies, Reichert et al. [47] prepared IrO<sub>2</sub>-TiO<sub>2</sub> solid solutions using a modified Pechini sol-gel method. The research showed that Ir can promote the phase transition of TiO<sub>2</sub> from anatase to rutile. The IrO<sub>2</sub>-TiO<sub>2</sub> solid solutions demonstrated significantly enhanced conductivity (Figure 8b,c), even at low levels of Ir doping.

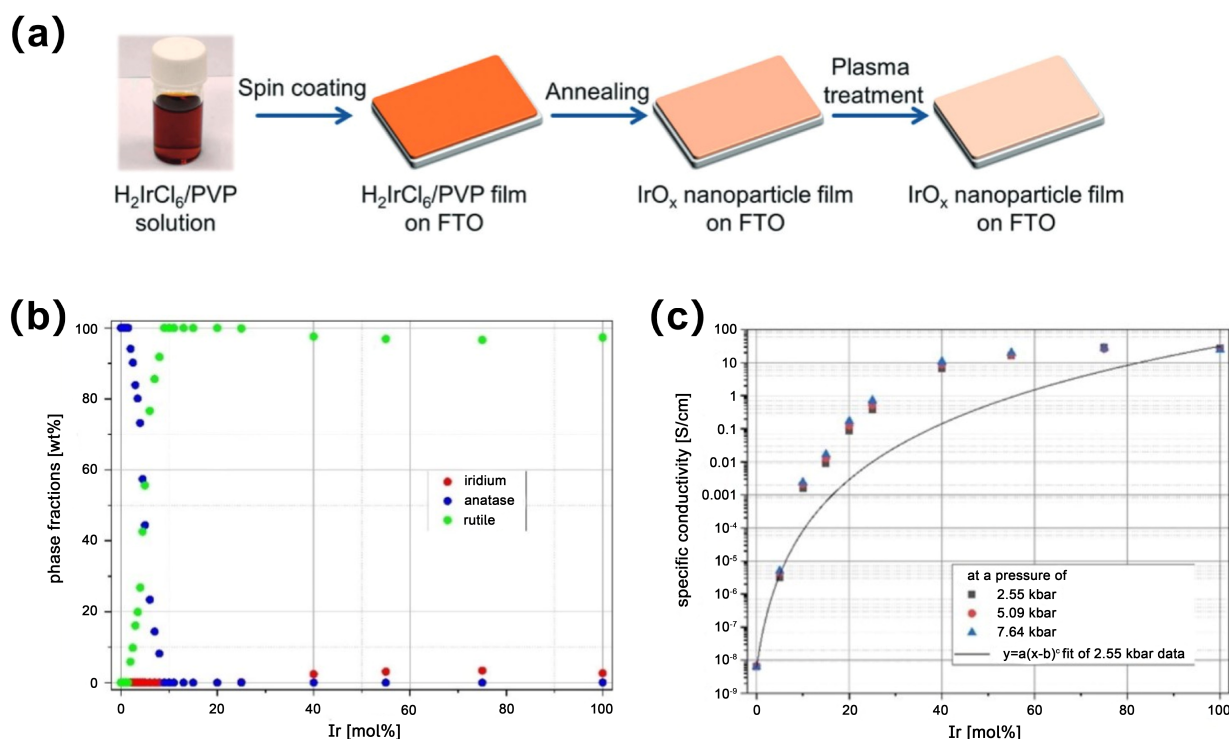


**Figure 8.** (a) Schematic illustration of the preparation of IrO<sub>x</sub> nanoparticle films on FTO [128]. (b) Phase fractions of the doping series Ir<sub>x</sub>Ti<sub>1-x</sub>O<sub>2</sub> synthesized via a modified Pechini sol-gel route after calcination at T = 400 °C. (c) Logarithmic representations of the specific conductivities of powder samples according to the two-point method of the doping series Ir<sub>x</sub>Ti<sub>1-x</sub>O<sub>2</sub> prepared via a modified Pechini sol-gel route after calcination at T = 400 °C [47].

Future research on the sol-gel method should focus on further optimizing the preparation process to achieve more efficient and stable IrO<sub>2</sub> film catalysts. This includes exploring lower temperature, heat treatment conditions, and developing new precursors and solvent systems, and may have a greater impact on hydrogen production through water electrolysis and other energy conversion fields.

### 3.5. Other Methods

In the one-step fabrication of IrO<sub>2</sub> catalysts for OER electrodes, besides electrochemical deposition, CVD, and PVD, several other common methods include atomic layer deposition (ALD), self-assembly [129,130], solution dipping [131], and spray pyrolysis [132,133].

ALD is a thin film deposition technique based on surface-limited reactions. This process involves the alternating introduction of precursors and reactants onto the substrate surface, enabling stepwise chemical reactions to achieve layer-by-layer deposition of materials. The “one-step film formation” process for fabricating IrO<sub>2</sub> films using ALD comprises several critical steps: first, precursor molecules are introduced and uniformly adsorbed onto the substrate surface; next, a first purge is conducted to remove any unreacted precursor molecules; then, an oxidizing agent is introduced to react with the adsorbed precursor, forming a layer of IrO<sub>2</sub> film; finally, a second purge is performed to eliminate any residual reaction byproducts. This layer-by-layer deposition approach ensures the uniformity of the

film and precise control over its thickness, while also enhancing the adhesion between the film and the substrate.

This high-quality deposition film presents significant advantages in catalytic applications. The strong adhesion ensures the stability of the catalyst under high current density and long-term operation. Consequently, ALD has garnered considerable attention in the preparation of catalysts. In terms of specific applications, Matienzo et al. [25] used ALD to prepare IrO<sub>2</sub> and NiO films (thickness < 60 nm) on Ni substrates. These crystalline films showed good activity for the OER process (Figure 9a), but were only active under high temperature and high pH conditions. Combining PLD technology with other techniques for the preparation of iridium-based films is also a good strategy. Park et al. [134] reported using plasma-enhanced atomic layer deposition (PEALD) to deposit Ir films on three-dimensional electrodes. As shown in Figure 9b, the deposited electrodes exhibited good step coverage and electrical performance. Despite the significant advantages of ALD in thin film deposition, the performance of the films largely depends on the choice of substrate material and the film growth mode. Extremely thin iridium layers are highly dependent on the substrate material. Schmitt et al. [78] evaluated the nucleation, film growth, and layer characteristics of iridium films prepared by ALD on substrates such as SiO<sub>2</sub>, TiO<sub>2</sub>, Ta<sub>2</sub>O<sub>5</sub>, Al<sub>2</sub>O<sub>3</sub>, Cr, Mo, and graphite. The study found that iridium exhibited an island growth mode (Volmer–Weber growth) on all substrate materials (Figure 9c). Ideal nucleation and growth of iridium were observed on TiO<sub>2</sub> and Ta<sub>2</sub>O<sub>5</sub> substrates, while good adhesion was seen on Al<sub>2</sub>O<sub>3</sub>, Cr, and carbon substrates. Iridium tended to peel off on other substrates. Iridium films on TiO<sub>2</sub> showed the lowest specific resistivity ( $7.7 \times 10^{-8} \Omega \cdot \text{m}$ ), which is crucial for OER. Based on these results, targeted selection of electrode substrate materials can achieve the best catalytic performance for the OER.

The self-assembly method relies on non-covalent interactions (such as electrostatic interactions, hydrogen bonding, van der Waals forces, etc.) between molecules or nanoparticles. Through these interactions, molecules or nanoparticles arrange themselves on surfaces or interfaces to form ordered structures with high order and consistency. The steps for achieving one-step film formation via self-assembly include preparing the solution, treating the substrate, performing self-assembly in the solution, removing excess solution and cleaning, and drying and curing the film. By adjusting self-assembly conditions (such as concentration, solution composition, temperature, substrate properties, etc.), the structure and thickness of the films can be controlled. Yagi et al. [129] formed a monolayer of colloidal particles on ITO electrodes via the self-assembly of citrate-stabilized IrO<sub>2</sub> colloids, significantly enhancing electrocatalytic water oxidation performance. This catalyst exhibited the highest TOF of  $(2.3\text{--}2.5) \times 10^4 \text{ h}^{-1}$  in neutral aqueous solutions. During the self-assembly process, the carboxyl groups of the citrate formed ester bonds with the hydroxyl groups on the ITO surface, achieving chemical adsorption. By adjusting the solution pH, the self-assembly of IrO<sub>2</sub> colloids was optimized, endowing the catalyst with high catalytic activity and excellent stability in electrocatalytic water oxidation reactions. Recently, the Cloward team [135] proposed a new mechanism for forming nanoscale aggregates through non-covalent self-assembly. The catalyst preparation involved dissolving monometallic iridium complexes and bimetallic iridium complexes with long-chain alkyl substituents in a solvent, then self-assembling into nanoscale aggregates through non-covalent interactions, significantly enhancing catalytic efficiency. Compared to monometallic catalysts, bimetallic iridium catalysts exhibited higher hydrogen evolution efficiency and lower overpotential in neutral aqueous solutions. The nanoscale aggregates formed through self-assembly placed multiple iridium centers in close proximity, effectively capturing light through the local high concentration of iridium atoms and promoting the coupling of bimetallic H-H bonds, thereby accelerating the photodriven electrocatalytic hydrogen evolution reaction in water. This research provides a new strategy for achieving efficient photodriven water splitting reactions under lower overpotentials and higher activity, which is of great significance for the optimization of the OER.

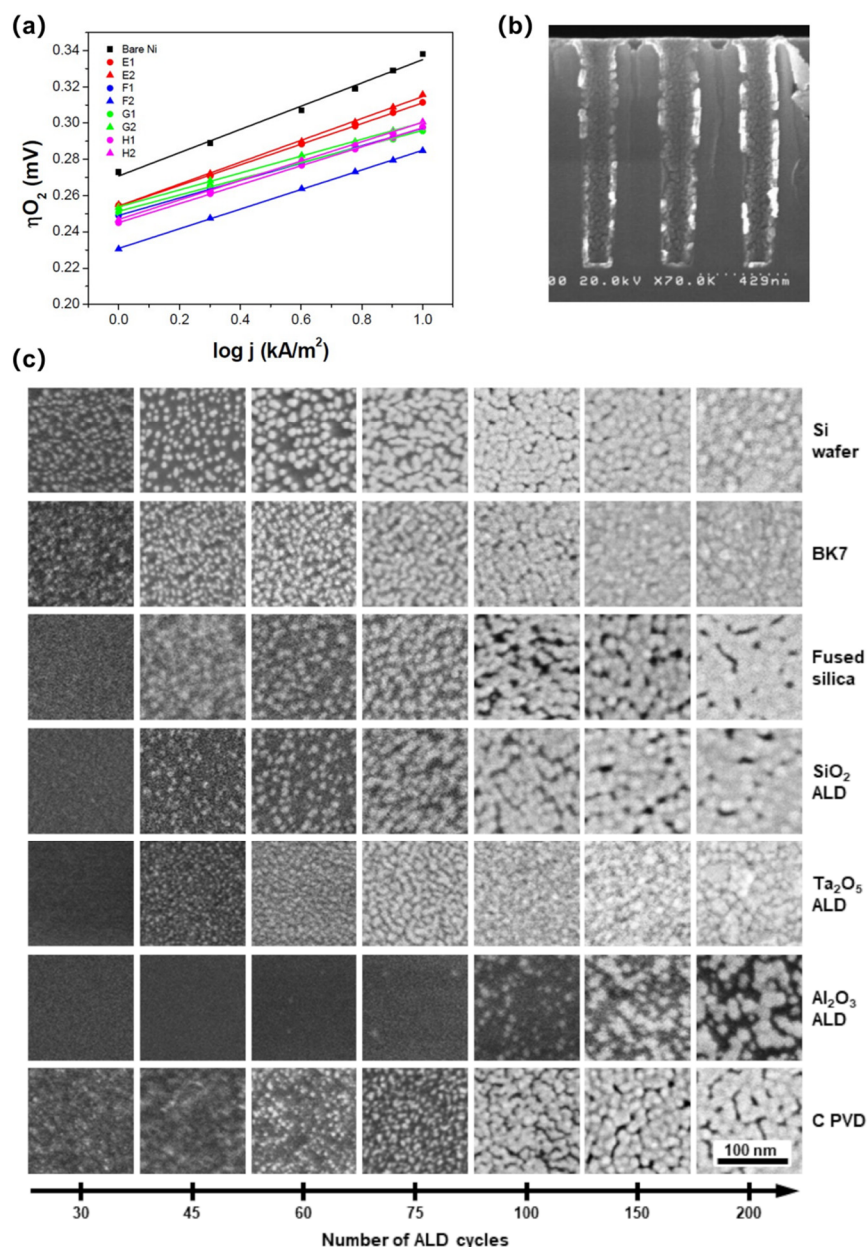


**Figure 9.** (a) Polarization curve (Tafel plot) of electrochemical oxygen evolution reaction (OER) of NiO thin film electrode [25]. (b) Cross-sectional SEM images of Ir films grown by PEALD [134]. (c) Scanning electron microscope (SEM) images (top-view) of iridium (Ir) coatings depending on the number of ALD cycles (columns) on Si wafers, BK7, and fused silica as well as seed layers of SiO<sub>2</sub>, Ta<sub>2</sub>O<sub>5</sub>, Al<sub>2</sub>O<sub>3</sub>, and C (rows). Iridium appears bright on the dark substrate materials. The scale bar in the bottom right corner is valid for all images [78].

In addition, several other methods are valuable for the preparation of IrO<sub>2</sub> films for OER but are not discussed in detail here due to space limitations. These methods include solution dipping, spray pyrolysis, and liquid phase deposition. Each of these techniques has unique characteristics and advantages that may offer distinct benefits for specific applications, warranting further research and exploration.

#### 4. Future Prospects

One-step film fabrication techniques demonstrate promising application prospects in the field of oxygen evolution reaction (OER) catalysis. Leveraging their unique advantages, these techniques can construct uniform and dense IrO<sub>2</sub> (iridium oxide) films in one step,



significantly enhancing their electrochemical performance and stability while effectively avoiding interface defects and structural inconsistencies that may arise from traditional multi-step preparation processes. Although the application of one-step fabrication for iridium oxide films in OER has achieved significant progress, there remains substantial room for optimization and further development. Future research could focus on the following areas: I. Development of Iridium-Based High-Entropy Alloy Films: Investigate how the complex compositions of high-entropy alloys influence catalytic performance, and optimize the activity and stability of iridium-based films by adjusting the elemental composition, thereby enhancing their OER catalytic efficiency. II. Iridium-Doped Metal Oxide Films: Utilize iridium doping techniques to modulate the electronic structure and surface activity of metal oxide films, further optimizing OER performance. This approach is particularly significant for improving catalyst durability and reducing costs. III. Films with Iridium Supported on High-Porosity Materials: By loading iridium onto high-porosity materials (such as porous carbon or metal–organic frameworks, MOFs), the specific surface area and electrical conductivity of the films can be increased, significantly improving OER catalytic efficiency and material utilization. IV. Application of Iridium in Nanotube and Nanocage Structures: Explore the application of iridium-based films in nanotube and nanocage structures, which can provide a larger specific surface area and more active sites, thereby further enhancing catalytic performance. V. Fabrication and Application of Iridium-Based Two-Dimensional Materials: Develop films of iridium-loaded two-dimensional materials (such as graphene and other two-dimensional transition metal dichalcogenides) to exploit their excellent conductivity and surface properties, further enhancing OER performance. VI. Design of Catalysts with Self-Repair Mechanisms: Research  $\text{IrO}_2$  catalysts with self-repair capabilities that can reconstruct or migrate during prolonged electrolysis to repair active site loss or surface damage caused by redox reactions, thereby extending the catalyst's lifespan and improving stability. VII. Integrated Multiscale Theoretical and Experimental Studies: Combine theoretical simulations with experimental research to deepen the understanding of the catalytic mechanisms of iridium oxide films, providing guidance for the design and synthesis of novel catalytic materials.

## 5. Summary

By exploring these directions in greater depth, the design and fabrication techniques for iridium oxide film catalysts will continue to improve in the future. These advancements will not only significantly enhance the efficiency and stability of the OER but also promote their key roles in a broader range of applications. Such research will help address global energy challenges, foster further development of clean energy technologies, and provide a rich theoretical basis and technical support for the development and innovation of new materials. In the future, with continuous technological breakthroughs and the advancement of materials science, we anticipate that these advanced  $\text{IrO}_2$  catalysts will demonstrate even stronger performance and longer service life in practical applications, contributing more significantly to the realization of sustainable energy.

**Author Contributions:** Conceptualization, W.L.; writing—review and editing, W.L., J.Z. and H.C.; methodology, Z.T.; supervision, X.W. (Xian Wang); validation, Y.W.; formal analysis, X.W. (Xingqiang Wang) and C.H.; visualization, X.Z. (Xingdong Zhao) and X.Z. (Xuxiang Zhang). All authors have read and agreed to the published version of the manuscript.

**Funding:** This research was funded by the National Science Foundation of China (Nos. 52061019 and 52161005), Scientific and Technological Project of Yunnan Precious Metals Laboratory (No. YPML-2022050214), The central government guides local funds for the development of science and technology (No. 202307AA110003), and Yunnan Science and Technology Projects (No. 202302AB080021 and 202203ZA080001).

**Institutional Review Board Statement:** Not applicable.

**Informed Consent Statement:** Not applicable.

**Data Availability Statement:** No new data were created or analyzed in this study. Data sharing is not applicable to this article.

**Conflicts of Interest:** The authors declare no conflict of interest.

## References

1. Raveendran, A.; Chandran, M.; Dhanusuraman, R. A Comprehensive Review on the Electrochemical Parameters and Recent Material Development of Electrochemical Water Splitting Electrocatalysts. *RSC Adv.* **2023**, *13*, 3843–3876. [[CrossRef](#)] [[PubMed](#)]
2. He, Y.; Liu, W.; Liu, J. MOF-Based/Derived Catalysts for Electrochemical Overall Water Splitting. *J. Colloid Interface Sci.* **2024**, *661*, 409–435. [[CrossRef](#)]
3. Qian, Q.; Zhu, Y.; Ahmad, N.; Feng, Y.; Zhang, H.; Cheng, M.; Liu, H.; Xiao, C.; Zhang, G.; Xie, Y. Recent Advancements in Electrochemical Hydrogen Production via Hybrid Water Splitting. *Adv. Mater.* **2024**, *36*, 2306108. [[CrossRef](#)] [[PubMed](#)]
4. Peng, D.D.; Fowler, M.; Elkamel, A.; Almansoori, A.; Walker, S.B. Enabling Utility-Scale Electrical Energy Storage by a Power-to-Gas Energy Hub and Underground Storage of Hydrogen and Natural Gas. *J. Nat. Gas Sci. Eng.* **2016**, *35*, 1180–1199. [[CrossRef](#)]
5. Wang, Z.; Zhang, X.; Rezazadeh, A. Hydrogen Fuel and Electricity Generation from a New Hybrid Energy System Based on Wind and Solar Energies and Alkaline Fuel Cell. *Energy Rep.* **2021**, *7*, 2594–2604. [[CrossRef](#)]
6. Dong, H.; Guo, J.E.; Liu, J.; Meng, T.; Li, M.; Chen, X.; Li, N.; Alavi, H. Energy Generation and Storing Electrical Energy in an Energy Hybrid System Consisting of Solar Thermal Collector, Stirling Engine and Thermoelectric Generator. *Sustain. Cities Soc.* **2021**, *75*, 103357. [[CrossRef](#)]
7. Shiva Kumar, S.; Lim, H. An Overview of Water Electrolysis Technologies for Green Hydrogen Production. *Energy Rep.* **2022**, *8*, 13793–13813. [[CrossRef](#)]
8. Amini Horri, B.; Ozcan, H. Green Hydrogen Production by Water Electrolysis: Current Status and Challenges. *Curr. Opin. Green Sustain. Chem.* **2024**, *47*, 100932. [[CrossRef](#)]
9. Xu, Y.; Zhang, X.; Liu, Y.; Wang, R.; Yang, Y.; Chen, J. A Critical Review of Research Progress for Metal Alloy Materials in Hydrogen Evolution and Oxygen Evolution Reaction. *Environ. Sci. Pollut. Res.* **2023**, *30*, 11302–11320. [[CrossRef](#)]
10. Batchelor, T.A.A.; Pedersen, J.K.; Winther, S.H.; Castelli, I.E.; Jacobsen, K.W.; Rossmeisl, J. High-Entropy Alloys as a Discovery Platform for Electrocatalysis. *Joule* **2019**, *3*, 834–845. [[CrossRef](#)]
11. Zhang, K.; Zou, R. Advanced Transition Metal-Based OER Electrocatalysts: Current Status, Opportunities, and Challenges. *Small* **2021**, *17*, 2100129. [[CrossRef](#)]
12. Choudhury, D.; Das, R.; Maurya, R.; Kumawat, H.; Neergat, M. Kinetics of the Oxygen Evolution Reaction (OER) on Amorphous and Crystalline Iridium Oxide Surfaces in Acidic Medium. *Langmuir* **2023**, *39*, 13748–13757. [[CrossRef](#)] [[PubMed](#)]
13. Han, N.; Zhang, X.; Zhang, C.; Feng, S.; Zhang, W.; Guo, W.; Zheng, R.; Zheng, R.; Liu, P.; Li, Y.; et al. Lowering the Kinetic Barrier via Enhancing Electrophilicity of Surface Oxygen to Boost Acidic Oxygen Evolution Reaction. *Matter* **2024**, *7*, 1330–1343. [[CrossRef](#)]
14. Naito, T.; Shinagawa, T.; Nishimoto, T.; Takanebe, K. Recent Advances in Understanding Oxygen Evolution Reaction Mechanisms over Iridium Oxide. *Inorg. Chem. Front.* **2021**, *8*, 2900–2917. [[CrossRef](#)]
15. Wu, H.; Wang, Y.; Shi, Z.; Wang, X.; Yang, J.; Xiao, M.; Ge, J.; Xing, W.; Liu, C. Recent Developments of Iridium-Based Catalysts for the Oxygen Evolution Reaction in Acidic Water Electrolysis. *J. Mater. Chem. A* **2022**, *10*, 13170–13189. [[CrossRef](#)]
16. Ledendecker, M.; Geiger, S.; Hengge, K.; Lim, J.; Cherevko, S.; Mingers, A.M.; Göhl, D.; Fortunato, G.V.; Jalalpoor, D.; Schüth, F.; et al. Towards Maximized Utilization of Iridium for the Acidic Oxygen Evolution Reaction. *Nano Res.* **2019**, *12*, 2275–2280. [[CrossRef](#)]
17. Chen, X.; Niu, K.; Xue, Z.; Liu, X.; Liu, B.; Zhang, B.; Zeng, H.; Lv, W.; Zhang, Y.; Wu, Y. Ultrafine Platinum Nanoparticles Supported on N,S-Codoped Porous Carbon Nanofibers as Efficient Multifunctional Materials for Noticeable Oxygen Reduction Reaction and Water Splitting Performance. *Nanoscale Adv.* **2022**, *4*, 1639–1648. [[CrossRef](#)]
18. Reier, T.; Oezaslan, M.; Strasser, P. Electrocatalytic Oxygen Evolution Reaction (OER) on Ru, Ir, and Pt Catalysts: A Comparative Study of Nanoparticles and Bulk Materials. *ACS Catal.* **2012**, *2*, 1765–1772. [[CrossRef](#)]
19. Zhang, Y.; Zhu, X.; Zhang, G.; Shi, P.; Wang, A.-L. Rational Catalyst Design for Oxygen Evolution under Acidic Conditions: Strategies toward Enhanced Electrocatalytic Performance. *J. Mater. Chem. A* **2021**, *9*, 5890–5914. [[CrossRef](#)]
20. Qin, D.-D.; Tang, Y.; Ma, G.; Qin, L.; Tao, C.-L.; Zhang, X.; Tang, Z. Molecular Metal Nanoclusters for ORR, HER and OER: Achievements, Opportunities and Challenges. *Int. J. Hydrogen Energy* **2021**, *46*, 25771–25781. [[CrossRef](#)]
21. Cherevko, S.; Reier, T.; Zeradjanin, A.R.; Pawolek, Z.; Strasser, P.; Mayrhofer, K.J.J. Stability of Nanostructured Iridium Oxide Electrocatalysts during Oxygen Evolution Reaction in Acidic Environment. *Electrochem. Commun.* **2014**, *48*, 81–85. [[CrossRef](#)]
22. Xie, Z.; Liang, X.; Kang, Z.; Zou, Y.; Wang, X.; Wu, Y.A.; King, G.; Liu, Q.; Huang, Y.; Zhao, X.; et al. High-Porosity, Layered Iridium Oxide as an Efficient, Durable Anode Catalyst for Water Splitting. *CCS Chem.* **2024**. [[CrossRef](#)]
23. Tachikawa, T.; Beniya, A.; Shigetoh, K.; Higashi, S. Relationship Between OER Activity and Annealing Temperature of Sputter-Deposited Flat IrO<sub>2</sub> Thin Films. *Catal. Lett.* **2020**, *150*, 1976–1984. [[CrossRef](#)]

24. Frisch, M.; Raza, M.H.; Ye, M.-Y.; Sachse, R.; Paul, B.; Gunder, R.; Pinna, N.; Kraehnert, R. ALD-Coated Mesoporous Iridium-Titanium Mixed Oxides: Maximizing Iridium Utilization for an Outstanding OER Performance. *Adv. Mater. Interfaces* **2022**, *9*, 2102035. [[CrossRef](#)]
25. Matienzo, D.D.; Settipani, D.; Instuli, E.; Kallio, T. Active IrO<sub>2</sub> and NiO Thin Films Prepared by Atomic Layer Deposition for Oxygen Evolution Reaction. *Catalysts* **2020**, *10*, 92. [[CrossRef](#)]
26. Mei, B.; Seger, B.; Pedersen, T.; Malizia, M.; Hansen, O.; Chorkendorff, I.; Vesborg, P.C.K. Protection of P+-n-Si Photoanodes by Sputter-Deposited Ir/IrO<sub>x</sub> Thin Films. *J. Phys. Chem. Lett.* **2014**, *5*, 1948–1952. [[CrossRef](#)]
27. Strickler, A.L.; Flores, R.A.; King, L.A.; Nørskov, J.K.; Bajdich, M.; Jaramillo, T.F. Systematic Investigation of Iridium-Based Bimetallic Thin Film Catalysts for the Oxygen Evolution Reaction in Acidic Media. *ACS Appl. Mater. Interfaces* **2019**, *11*, 34059–34066. [[CrossRef](#)]
28. Özer, E.; Pawolek, Z.; Kühl, S.; Nong, H.N.; Paul, B.; Selve, S.; Spöri, C.; Bernitzky, C.; Strasser, P. Metallic Iridium Thin-Films as Model Catalysts for the Electrochemical Oxygen Evolution Reaction (OER)—Morphology and Activity. *Surfaces* **2018**, *1*, 151–164. [[CrossRef](#)]
29. Cherevko, S.; Geiger, S.; Kasian, O.; Kulyk, N.; Grote, J.-P.; Savan, A.; Shrestha, B.R.; Merzlikin, S.; Breitbach, B.; Ludwig, A.; et al. Oxygen and Hydrogen Evolution Reactions on Ru, RuO<sub>2</sub>, Ir, and IrO<sub>2</sub> Thin Film Electrodes in Acidic and Alkaline Electrolytes: A Comparative Study on Activity and Stability. *Catal. Today* **2016**, *262*, 170–180. [[CrossRef](#)]
30. Buvat, G.; Eslamibidgoli, M.J.; Garbarino, S.; Eikerling, M.; Guay, D. OER Performances of Cationic Substituted (100)-Oriented IrO<sub>2</sub> Thin Films: A Joint Experimental and Theoretical Study. *ACS Appl. Energy Mater.* **2020**, *3*, 5229–5237. [[CrossRef](#)]
31. Ding, L.; Li, K.; Wang, W.; Xie, Z.; Yu, S.; Yu, H.; Cullen, D.A.; Keane, A.; Ayers, K.; Capuano, C.B.; et al. Amorphous Iridium Oxide-Integrated Anode Electrodes with Ultrahigh Material Utilization for Hydrogen Production at Industrial Current Densities. *Nano-Micro Lett.* **2024**, *16*, 203. [[CrossRef](#)] [[PubMed](#)]
32. Petkucheva, E.; Borisov, G.; Lefterova, E.; Heiss, J.; Schnakenberg, U.; Slavcheva, E. Gold-Supported Magnetron Sputtered Ir Thin Films as OER Catalysts for Cost-Efficient Water Electrolysis. *Int. J. Hydrogen Energy* **2018**, *43*, 16905–16912. [[CrossRef](#)]
33. Choe, S.; Lee, B.-S.; Cho, M.K.; Kim, H.-J.; Henkensmeier, D.; Yoo, S.J.; Kim, J.Y.; Lee, S.Y.; Park, H.S.; Jang, J.H. Electrodeposited IrO<sub>2</sub>/Ti Electrodes as Durable and Cost-Effective Anodes in High-Temperature Polymer-Membrane-Electrolyte Water Electrolyzers. *Appl. Catal. B Environ.* **2018**, *226*, 289–294. [[CrossRef](#)]
34. Lee, K.; Flores, R.A.; Liu, Y.; Wang, B.Y.; Hikita, Y.; Sinclair, R.; Bajdich, M.; Hwang, H.Y. Epitaxial Stabilization and Oxygen Evolution Reaction Activity of Metastable Columbite Iridium Oxide. *ACS Appl. Energy Mater.* **2021**, *4*, 3074–3082. [[CrossRef](#)]
35. Zhao, F.; Wen, B.; Niu, W.; Chen, Z.; Yan, C.; Selloni, A.; Tully, C.G.; Yang, X.; Koel, B.E. Increasing Iridium Oxide Activity for the Oxygen Evolution Reaction with Hafnium Modification. *J. Am. Chem. Soc.* **2021**, *143*, 15616–15623. [[CrossRef](#)]
36. Hakimi, F.; Ghalkhani, M.; Rashchi, F.; Dolati, A. Pulse Electrodeposition Synthesis of Ti/PbO<sub>2</sub>-IrO<sub>2</sub> Nano-Composite Electrode to Restrict the OER in the Zinc Electrowinning. *J. Environ. Chem. Eng.* **2024**, *12*, 111985. [[CrossRef](#)]
37. Cheng, Y.; Yang, F.; Gong, J.; Wu, B.; Zhang, Z.; Chu, J. Platinum Nanoparticles Decorated IrO<sub>2</sub> @MWCNT as an Improved Catalyst for Oxygen Evolution Reaction. *ChemistrySelect* **2021**, *6*, 7542–7550. [[CrossRef](#)]
38. Liu, B.; Li, G.; Cai, X.; Wang, Y.; Zeng, Y.; Ren, Q.; Li, J. IrO<sub>2</sub> Nanoparticles Supported on Submicrometer-Sized TiO<sub>2</sub> as an Efficient and Stable Coating for Oxygen Evolution Reaction. *Electrochim. Acta* **2024**, *493*, 144392. [[CrossRef](#)]
39. Yoo, P.; Woo, M.; Lee, H.I.; Kim, H.S.; Lim, D.-H. Fabrication of Well-Dispersed IrO<sub>2</sub> Anchored on rGO Composite for High-Performance OER Electrocatalyst Application by Microwave-Assisted Method. *Electrocatalysis* **2023**, *14*, 891–900. [[CrossRef](#)]
40. Wang, Y.; Zhao, Z.; Liang, X.; Zhao, X.; Wang, X.; Jana, S.; Wu, Y.A.; Zou, Y.; Li, L.; Chen, H.; et al. Supported IrO<sub>2</sub> Nanocatalyst with Multilayered Structure for Proton Exchange Membrane Water Electrolysis. *Adv. Mater.* **2024**, 2407717. [[CrossRef](#)]
41. Wang, M.; Zhu, W.; Ma, M.; Fan, Z.; Yang, J.; Liao, F.; Shao, M. Lattice Strain Enhances the Activity of Ir-IrO<sub>2</sub>/C for Acidic Oxygen Evolution Reaction. *ChemElectroChem* **2022**, *9*, e202200732. [[CrossRef](#)]
42. Joshi, P.; Yadav, R.; Hara, M.; Inoue, T.; Motoyama, Y.; Yoshimura, M. Contribution of BN-Co-Doped Reduced Graphene Oxide as a Catalyst Support on Activity of Iridium Oxide for Oxygen Evolution Reaction. *J. Mater. Chem. A* **2021**. [[CrossRef](#)]
43. Li, H.; Xu, Y.; Lv, N.; Zhang, Q.; Zhang, X.; Wei, Z.; Wang, Y.; Tang, H.; Pan, H. Ti-Doped SnO<sub>2</sub> Supports IrO<sub>2</sub> Electrocatalysts for the Oxygen Evolution Reaction (OER) in PEM Water Electrolysis. *ACS Sustain. Chem. Eng.* **2023**, *11*, 1121–1132. [[CrossRef](#)]
44. Han, W.; Qian, Y.; Zhang, F.; He, Y.; Li, P.; Zhang, X. 1 Ultrasmall IrO<sub>2</sub> Nanoparticles Anchored on 2 Hollow Co-Mo Multi-Oxide Heterostructure 3 Nanocages for Efficient Oxygen Evolution in 4 Acid. *Chem. Eng. J.* **2023**, *473*, 145353. [[CrossRef](#)]
45. Cao, H.; Chen, M.; Wu, L.; Hou, G.; Tang, Y.; Zheng, G. Electrochemical Properties of IrO<sub>2</sub> Active Anode with TNIs Interlayer for Oxygen Evolution. *Appl. Surf. Sci.* **2018**, *428*, 861–869. [[CrossRef](#)]
46. Osaka, A.; Takatsuna, T.; Miura, Y. Iridium Oxide Films via Sol-Gel Processing. *J. Non-Cryst. Solids* **1994**, *178*, 313–319. [[CrossRef](#)]
47. Reichert, D.; Stöwe, K. Sol-Gel-Syntheses and Structural as Well as Electrical Characterizations of Anatase- and Rutile-Type Solid Solutions in the System IrO<sub>2</sub>-TiO<sub>2</sub>. *ChemistryOpen* **2023**, *12*, e202300032. [[CrossRef](#)]
48. Felix, C.; Bladergroen, B.J.; Linkov, V.; Pollet, B.G.; Pasupathi, S. Ex-Situ Electrochemical Characterization of IrO<sub>2</sub> Synthesized by a Modified Adams Fusion Method for the Oxygen Evolution Reaction. *Catalysts* **2019**, *9*, 318. [[CrossRef](#)]
49. Liu, Z.; Qi, J.; Zeng, H.; Zeng, Y.; Wang, J.; Gu, L.; Hong, E.; Yang, M.; Fu, Q.; Chen, J.; et al. Electrochemical Preparation of Iridium Hydroxide Nanosheets with Ordered Honeycomb Structures for the Oxygen Evolution Reaction in Acid. *ACS Appl. Energy Mater.* **2022**, *5*, 6869–6877. [[CrossRef](#)]

50. Hrbek, T.; Kúš, P.; Kosto, Y.; Rodríguez, M.G.; Matolínová, I. Magnetron-Sputtered Thin-Film Catalyst with Low-Ir-Ru Content for Water Electrolysis: Long-Term Stability and Degradation Analysis. *J. Power Sources* **2023**, *556*, 232375. [[CrossRef](#)]
51. Slavcheva, E.; Radev, I.; Bliznakov, S.; Topalov, G.; Andreev, P.; Budevski, E. Sputtered Iridium Oxide Films as Electrocatalysts for Water Splitting via PEM Electrolysis. *Electrochim. Acta* **2007**, *52*, 3889–3894. [[CrossRef](#)]
52. Parsons, G.N.; Clark, R.D. Area-Selective Deposition: Fundamentals, Applications, and Future Outlook. *Chem. Mater.* **2020**, *32*, 4920–4953. [[CrossRef](#)]
53. Ben-Naim, M.; Palm, D.W.; Strickler, A.L.; Nielander, A.C.; Sanchez, J.; King, L.A.; Higgins, D.C.; Jaramillo, T.F. A Spin Coating Method to Deposit Iridium-Based Catalysts onto Silicon for Water Oxidation Photoanodes. *ACS Appl. Mater. Interfaces* **2020**, *12*, 5901–5908. [[CrossRef](#)]
54. Reier, T.; Weidinger, I.; Hildebrandt, P.; Kraehnert, R.; Strasser, P. Electrocatalytic Oxygen Evolution Reaction on Iridium Oxide Model Film Catalysts: Influence of Oxide Type and Catalyst Substrate Interactions. *ECS Trans.* **2013**, *58*, 39. [[CrossRef](#)]
55. Chandra, D.; Sato, T.; Tanahashi, Y.; Takeuchi, R.; Yagi, M. Facile Fabrication and Nanostructure Control of Mesoporous Iridium Oxide Films for Efficient Electrocatalytic Water Oxidation. *Energy* **2019**, *173*, 278–289. [[CrossRef](#)]
56. Gao, J.; Xu, C.-Q.; Hung, S.-F.; Liu, W.; Cai, W.; Zeng, Z.; Jia, C.; Chen, H.M.; Xiao, H.; Li, J.; et al. Breaking Long-Range Order in Iridium Oxide by Alkali Ion for Efficient Water Oxidation. *J. Am. Chem. Soc.* **2019**, *141*, 3014–3023. [[CrossRef](#)] [[PubMed](#)]
57. Kasian, O.; Geiger, S.; Li, T.; Grote, J.-P.; Schweinar, K.; Zhang, S.; Scheu, C.; Raabe, D.; Cherevko, S.; Gault, B.; et al. Degradation of Iridium Oxides via Oxygen Evolution from the Lattice: Correlating Atomic Scale Structure with Reaction Mechanisms. *Energy Environ. Sci.* **2019**, *12*, 3548–3555. [[CrossRef](#)]
58. Wang, C.; Schechter, A.; Feng, L. Iridium-Based Catalysts for Oxygen Evolution Reaction in Acidic Media: Mechanism, Catalytic Promotion Effects and Recent Progress. *Nano Res. Energy* **2023**, *2*, e9120056. [[CrossRef](#)]
59. Saveleva, V.A.; Wang, L.; Teschner, D.; Jones, T.; Gago, A.S.; Friedrich, K.A.; Zafeiratos, S.; Schlögl, R.; Savinova, E.R. Operando Evidence for a Universal Oxygen Evolution Mechanism on Thermal and Electrochemical Iridium Oxides. *J. Phys. Chem. Lett.* **2018**, *9*, 3154–3160. [[CrossRef](#)]
60. Ding, Y.; Liu, W.; Xu, Z.; Duan, Z. The Origin of High Electrochemical Stability of Iridium Oxides for Oxygen Evolution. *J. Mater. Chem. A* **2024**, *12*, 20317–20326. [[CrossRef](#)]
61. Lin, Z.; Wang, T.; Li, Q. Designing Active and Stable Ir-Based Catalysts for the Acidic Oxygen Evolution Reaction. *Ind. Chem. Mater.* **2023**, *1*, 299–311. [[CrossRef](#)]
62. Wang, X.; Zhong, H.; Xi, S.; Lee, W.S.V.; Xue, J. Understanding of Oxygen Redox in the Oxygen Evolution Reaction. *Adv. Mater.* **2022**, *34*, 2107956. [[CrossRef](#)]
63. Xu, J.; Jin, H.; Lu, T.; Li, J.; Liu, Y.; Davey, K.; Zheng, Y.; Qiao, S.-Z. IrO<sub>x</sub>·nH<sub>2</sub>O with Lattice Water-Assisted Oxygen Exchange for High-Performance Proton Exchange Membrane Water Electrolyzers. *Sci. Adv.* **2023**, *9*, eadh1718. [[CrossRef](#)]
64. Zhao, M.; Feng, J.; Li, Z.; Zou, Z. Lattice Water Fuels Acidic Water Oxidation. *Sci. China Chem.* **2024**, *67*, 2132–2133. [[CrossRef](#)]
65. Schwarzacher, W. Electrodeposition: A Technology for the Future. *Electrochem. Soc. Interface* **2006**, *15*, 32–33. [[CrossRef](#)]
66. Wu, D.; Wang, X.; Wu, X. A Study on the Anodic Electrodeposition of Iridium Oxide on Different Substrates. *J. Electrochem. Soc.* **2022**, *169*, 092503. [[CrossRef](#)]
67. Lee, B.-S.; Ahn, S.H.; Park, H.-Y.; Choi, I.; Yoo, S.J.; Kim, H.-J.; Henkensmeier, D.; Kim, J.Y.; Park, S.; Nam, S.W.; et al. Development of Electrodeposited IrO<sub>2</sub> Electrodes as Anodes in Polymer Electrolyte Membrane Water Electrolysis. *Appl. Catal. B-Environ.* **2015**, *179*, 285–291. [[CrossRef](#)]
68. Jeong, H.-Y.; Oh, J.; Yi, G.S.; Park, H.-Y.; Cho, S.K.; Jang, J.H.; Yoo, S.J.; Park, H.S. High-Performance Water Electrolyzer with Minimum Platinum Group Metal Usage: Iron Nitride-Iridium Oxide Core-Shell Nanostructures for Stable and Efficient Oxygen Evolution Reaction. *Appl. Catal. B Environ.* **2023**, *330*, 122596. [[CrossRef](#)]
69. Nga Ngo (Sarah Ngo), T.H.; Love, J.; O'Mullane, A.P. Investigating the Influence of Amorphous/Crystalline Interfaces on the Stability of IrO<sub>2</sub> for the Oxygen Evolution Reaction in Acidic Electrolyte. *ChemElectroChem* **2023**, *10*, e202300438. [[CrossRef](#)]
70. Cho, J.; Kim, K.-S.; Kim, S.; Shao, Y.; Kim, Y.-T.; Park, S. Substrate-Driven Catalyst Reducibility for Oxygen Evolution and Its Effect on the Operation of Proton Exchange Membrane Water Electrolyzers. *Small Struct.* **2024**, *5*, 2300276. [[CrossRef](#)]
71. Abyaneh, M.Y.; Fleischmann, M. General Models for Surface Nucleation and Three-Dimensional Growth: The Effects of Concurrent Redox Reactions and of Diffusion. *J. Electrochem. Soc.* **1991**, *138*, 2491. [[CrossRef](#)]
72. Reier, T.; Teschner, D.; Lunkenbein, T.; Bergmann, A.; Selve, S.; Kraehnert, R.; Schlögl, R.; Strasser, P. Electrocatalytic Oxygen Evolution on Iridium Oxide: Uncovering Catalyst-Substrate Interactions and Active Iridium Oxide Species. *J. Electrochem. Soc.* **2014**, *161*, F876. [[CrossRef](#)]
73. Schneider, C.W.; Esposito, M.; Marozau, I.; Conder, K.; Doebeli, M.; Hu, Y.; Mallepell, M.; Wokaun, A.; Lippert, T. The Origin of Oxygen in Oxide Thin Films: Role of the Substrate. *Appl. Phys. Lett.* **2010**, *97*, 192107. [[CrossRef](#)]
74. Oyshi, T.A.; Islam, M.T.; Al-Humaidi, J.Y.; Rahman, M.M.; Hasnat, M.A. Nanoarchitectonics for Optimization of a Ti/Au-IrO<sub>x</sub> Electrode for Enhanced Catalytic Performance Pertinent to Hydrogen Evolution Reaction. *Int. J. Hydrogen Energy* **2024**, *64*, 1011–1020. [[CrossRef](#)]
75. Kumar, S.A.; Sahoo, S.; Laxminarayana, G.K.; Rout, C.S. Electrochemical Deposition for Cultivating Nano- and Microstructured Electroactive Materials for Supercapacitors: Recent Developments and Future Perspectives. *Small* **2024**. [[CrossRef](#)]
76. Therese, G.H.A.; Kamath, P.V. Electrochemical Synthesis of Metal Oxides and Hydroxides. *Chem. Mater.* **2000**, *12*, 1195–1204. [[CrossRef](#)]

77. Petit, M.A.; Plichon, V. Anodic Electrodeposition of Iridium Oxide Films. *J. Electroanal. Chem.* **1998**, *444*, 247–252. [CrossRef]
78. Schmitt, P.; Beladiya, V.; Felde, N.; Paul, P.; Otto, F.; Fritz, T.; Tünnermann, A.; Szeghalmi, A.V. Influence of Substrate Materials on Nucleation and Properties of Iridium Thin Films Grown by ALD. *Coatings* **2021**, *11*, 173. [CrossRef]
79. Wu, W.; Chen, Z. Iridium Coating: Processes, Properties and Application. Part I. Available online: <https://www.ingentaconnect.com/content/matthey/jmtr/2017/00000061/00000001/art00004> (accessed on 3 August 2024).
80. El Khakani, M.A.; Chaker, M.; Le Drogoff, B. Iridium Thin Films Deposited by Radio-Frequency Magnetron Sputtering. *J. Vac. Sci. Technol. A* **1998**, *16*, 885–888. [CrossRef]
81. Negi, S.; Bhandari, R.; Rieth, L.; Solzbacher, F. Effect of Sputtering Pressure on Pulsed-DC Sputtered Iridium Oxide Films. *Sens. Actuators B Chem.* **2009**, *137*, 370–378. [CrossRef]
82. Geiger, S.; Kasian, O.; Shrestha, B.R.; Mingers, A.M.; Mayrhofer, K.J.J.; Cherevko, S. Activity and Stability of Electrochemically and Thermally Treated Iridium for the Oxygen Evolution Reaction. *J. Electrochem. Soc.* **2016**, *163*, F3132. [CrossRef]
83. Buvat, G.; Eslamibidgoli, M.J.; Youssef, A.H.; Garbarino, S.; Ruediger, A.; Eikerling, M.; Guay, D. Effect of IrO<sub>6</sub> Octahedron Distortion on the OER Activity at (100) IrO<sub>2</sub> Thin Film. *ACS Catal.* **2020**, *10*, 806–817. [CrossRef]
84. El Khakani, M.A.; Chaker, M. Reactive Pulsed Laser Deposition of Iridium Oxide Thin Films. *Thin Solid Film.* **1998**, *335*, 6–12. [CrossRef]
85. Wilson, A.A.; Graziano, M.B.; Leff, A.C.; Hanrahan, B.; Baker, D.R.; Rivas, M.; Sanchez, B.; Parker, T.; Sunal, P. Growth Conditions and Mechanisms for IrOx Nano-Platelet Formation by Reactive Sputtering. *J. Cryst. Growth* **2022**, *577*, 126374. [CrossRef]
86. Laguna-Marco, M.A.; Herrero-Albillos, J.; Aguirre, M.H.; Rueda-Jimenez, M.; Mikulska, I. Novel Ir<sub>1-x</sub>Co<sub>x</sub>O<sub>2</sub> Thin Films: Growth and Characterization. *J. Alloy. Compd.* **2023**, *968*, 171975. [CrossRef]
87. Slavcheva, E.P. Magnetron Sputtered Iridium Oxide as Anode Catalyst for Pem Hydrogen Generation. *Maced. J. Chem. Chem. Eng.* **2011**, *30*, 45–54. [CrossRef]
88. Khoa, T.D.; Horii, S.; Horita, S. High Deposition Rate of Epitaxial (100) Iridium Film on (100)YSZ/(1 0 0)Si Substrate by RF Sputtering Deposition. *Thin Solid Film.* **2002**, *419*, 88–94. [CrossRef]
89. Kang, X.; Liu, J.; Tian, H.; Yang, B.; NuLi, Y.; Yang, C. Optimization and Electrochemical Characterization of RF-Sputtered Iridium Oxide Microelectrodes for Electrical Stimulation. *J. Micromech. Microeng.* **2014**, *24*, 025015. [CrossRef]
90. Zenkin, S.; Gaydaychuk, A.; Linnik, S. Effects of Sputtering Gas on the Microstructure of Ir Thin Films Deposited by HiPIMS and Pulsed DC Sputtering. *Surf. Coat. Technol.* **2021**, *412*, 127038. [CrossRef]
91. Fang, Z.; Hu, Z.; Lv, B.; Sun, B.; Wang, H.; He, P.; Wang, X.; Liang, X.; Jin, G. The New Iridium-Hafnium-Aluminum Alloy Thin Films with Excellent Mechanical Properties and Oxidation Resistance. *Appl. Surf. Sci.* **2024**, *657*, 159802. [CrossRef]
92. Ohmori, T.; Go, H.; Nakayama, A.; Mametsuka, H.; Suzuki, E. Influence of Sputtering Parameters on Hydrogen Evolution Overvoltage in Sputter-Deposited Co–Mo Alloy Electrode. *Mater. Lett.* **2001**, *47*, 103–106. [CrossRef]
93. Li, C.; Hsieh, J.-H. Parameters and Stability Analysis of Reactive Sputtering. *Jpn. J. Appl. Phys.* **2003**, *42*, 6653. [CrossRef]
94. Slavcheva, E.; Schnakenberg, U.; Mokwa, W. Deposition of Sputtered Iridium Oxide—Influence of Oxygen Flow in the Reactor on the Film Properties. *Appl. Surf. Sci.* **2006**, *253*, 1964–1969. [CrossRef]
95. Reinhold, E.; Faber, J. Large Area Electron Beam Physical Vapor Deposition (EB-PVD) and Plasma Activated Electron Beam (EB) Evaporation—Status and Prospects. *Surf. Coat. Technol.* **2011**, *206*, 1653–1659. [CrossRef]
96. Matthews, L.R.; Parkhill, R.L.; Knobbe, E.T. Optical Characterization of Binary, Tertiary, and Quaternary II-VI Semiconductor Thin Films Prepared by Pulsed Excimer Laser Deposition. In Proceedings of the Excimer Lasers, Optics, and Applications, San Jose, CA, USA, 31 March 1997; SPIE: San Jose, CA, USA, 1997; Volume 2992, pp. 72–80.
97. Hou, X.; Takahashi, R.; Yamamoto, T.; Lippmaa, M. Microstructure Analysis of IrO<sub>2</sub> Thin Films. *J. Cryst. Growth* **2017**, *462*, 24–28. [CrossRef]
98. Hampden-Smith, M.J.; Kudas, T.T. Chemical Vapor Deposition of Metals: Part 1. An Overview of CVD Processes. *Chem. Vap. Depos.* **1995**, *1*, 8–23. [CrossRef]
99. Vasilyev, V.Y.; Morozova, N.B.; Basova, T.V.; Igumenov, I.K.; Hassan, A. Chemical Vapour Deposition of Ir-Based Coatings: Chemistry, Processes and Applications. *RSC Adv.* **2015**, *5*, 32034–32063. [CrossRef]
100. Sun, Y.-M.; Endle, J.P.; Smith, K.; Whaley, S.; Mahaffy, R.; Ekerdt, J.G.; White, J.M.; Hance, R.L. Iridium Film Growth with Indium Tris-Acetylacetonate: Oxygen and Substrate Effects. *Thin Solid Film.* **1999**, *346*, 100–107. [CrossRef]
101. Guerrero, R.M.; Torres, M.Z.F.; Zuñiga, I.M.M.; Estrada, E.M.A.; Garcia, J.R.V. Preparation and Characterization of Nanocrystalline Noble Metal Films by MOCVD. In *Proceedings of the Metastable, Mechanically Alloyed and Nanocrystalline Materials*; Inoue, A., Ed.; Trans Tech Publications Ltd.: Stafa-Zurich, Switzerland, 2005; Volume 24–25, pp. 623–626.
102. Zhang, F.; Barrowcliff, R.; Stecker, G.; Pan, W.; Wang, D.; Hsu, S.-T. Synthesis of Metallic Iridium Oxide Nanowires via Metal Organic Chemical Vapor Deposition. *Jpn. J. Appl. Phys.* **2005**, *44*, L398. [CrossRef]
103. Jürgensen, L.; Frank, M.; Pyeon, M.; Czypiel, L.; Mathur, S. Subvalent Iridium Precursors for Atom-Efficient Chemical Vapor Deposition of Ir and IrO<sub>2</sub> Thin Films. *Organometallics* **2017**, *36*, 2331–2337. [CrossRef]
104. Garcia, J.R.V.; Goto, T. Chemical Vapor Deposition of Iridium, Platinum, Rhodium and Palladium. *Mater. Trans.* **2003**, *44*, 1717–1728. [CrossRef]
105. Jürgensen, L.; Frank, M.; Graf, D.; Gessner, I.; Fischer, T.; Welter, K.; Jägermann, W.; Mathur, S. Nanostructured IrOx Coatings for Efficient Oxygen Evolution Reactions in PV-EC Setup. *Z. Für Phys. Chem.* **2020**, *234*, 911–924. [CrossRef]
106. Yan, X.; Zhang, Q.; Fan, X. New MOCVD Precursor for Iridium Thin Films Deposition. *Mater. Lett.* **2007**, *61*, 216–218. [CrossRef]

107. Xu, C.; Baum, T.H.; Rheingold, A.L. New Precursors for Chemical Vapor Deposition of Iridium. *Chem. Mater.* **1998**, *10*, 2329–2331. [[CrossRef](#)]
108. Maury, F.; Senocq, F. Iridium Coatings Grown by Metal–Organic Chemical Vapor Deposition in a Hot-Wall CVD Reactor. *Surf. Coat. Technol.* **2003**, *163–164*, 208–213. [[CrossRef](#)]
109. Hernández-Pérez, M.A.; Vargas-García, J.R.; Romero-Serrano, J.A. Diagramas de fase CVD para la preparación de películas de iridio. *Rev. De Metal.* **2002**, *38*, 30–37. [[CrossRef](#)]
110. Yan, X.; Zhang, Q.; Fan, X. A new precursor for metal organic chemical vapor deposition of iridium thin films. *Rare Met. Mat. Eng.* **2006**, *35*, 1129–1131.
111. Dougherty, G.M.; Sands, T.D.; Pisano, A.P. Microfabrication Using One-Step LPCVD Porous Polysilicon Films. *J. Microelectromechanical Syst.* **2003**, *12*, 418–424. [[CrossRef](#)]
112. Modreanu, M.; Tomozeiu, N.; Gartner, M.; Cosmin, P. Microstructural and Optical Properties of As-Deposited LPCVD Silicon Films. *Thin Solid Film.* **2001**, *383*, 254–257. [[CrossRef](#)]
113. Chao, H.; Wu, Y.T.; Wang, W.-C. Optical Thin Films Using LPCVD and Thermal Reoxidation Techniques. In Proceedings of the Optical Thin Films V: New Developments, SPIE, San Diego, CA, USA, 1 October 1997; Volume 3133, pp. 226–229. [[CrossRef](#)]
114. Gulleri, G.; Carpanese, C.; Cascarano, C.; Lodi, D.; Ninni, R.; Ottaviani, G. Deposition Temperature Determination of HDPCVD Silicon Dioxide Films. *Microelectron. Eng.* **2005**, *82*, 236–241. [[CrossRef](#)]
115. Lim, S.H.; Kim, H.S.; Jang, J.; Lee, C.H. Field Emission from Nanostructure Carbon Films. *Int. J. Mod. Phys. B* **2002**, *16*, 983–987. [[CrossRef](#)]
116. Liu, Y.; Wang, R.; Li, Z.; Wang, S.; Huang, Y.; Peng, W. Non-Switching to Switching Transferring Mechanism Investigation for Ag/SiO<sub>x</sub>/p-Si Structure with SiO<sub>x</sub> Deposited by HWCVD. *J. Phys. D Appl. Phys.* **2018**, *51*, 165102. [[CrossRef](#)]
117. Swain, B.P. The Structural Characterisation of HWCVD-Deposited Nanocrystalline Silicon Films. *S. Afr. J. Sci.* **2009**, *105*, 77–80. [[CrossRef](#)]
118. Mungkalasiri, J.; Bedel, L.; Emieux, F.; Cara, A.V.-D.; Freney, J.; Maury, F.; Renaud, F.N.R. Antibacterial Properties of TiO<sub>2</sub>–Cu Composite Thin Films Grown by a One Step DLICVD Process. *Surf. Coat. Technol.* **2014**, *242*, 187–194. [[CrossRef](#)]
119. Boisselier, G.; Maury, F.; Schuster, F. Growth of Chromium Carbide in a Hot Wall DLICVD Reactor. *J. Nanosci. Nanotechnol.* **2011**, *11*, 8289–8293. [[CrossRef](#)]
120. Manole, C.C.; Maury, F.; Demetrescu, I. Patterned PPy Polymer and PPy/Ag Nanocomposites Thin Films by Photo-DLICVD. *Phys. Procedia* **2013**, *46*, 46–55. [[CrossRef](#)]
121. Mineshige, A. Preparation of Dense Electrolyte Layer Using Dissociated Oxygen Electrochemical Vapor Deposition Technique. *Solid State Ion.* **2004**, *175*, 483–485. [[CrossRef](#)]
122. Rosestolato, D.; Neodo, S.; Ferro, S.; Battaglin, G.; Rigato, V.; Battisti, A.D. A Comparison between Structural and Electrochemical Properties of Iridium Oxide-Based Electrocatalysts Prepared by Sol-Gel and Reactive Sputtering Deposition. *J. Electrochem. Soc.* **2014**, *161*, E151. [[CrossRef](#)]
123. Reksten, A.; Moradi, F.; Seland, F.; Sunde, S. Iridium-Ruthenium Mixed Oxides for Oxygen Evolution Reaction Prepared by Pechini Synthesis. *ECS Trans.* **2014**, *58*, 39. [[CrossRef](#)]
124. Osman, J.R.; Crayston, J.A.; Pratt, A.; Richens, D.T. RuO<sub>2</sub>–TiO<sub>2</sub> Mixed Oxides Prepared from the Hydrolysis of the Metal Alkoxides. *Mater. Chem. Phys.* **2008**, *110*, 256–262. [[CrossRef](#)]
125. Green, L.M.; Meek, D.W. Synthesis, Characterization and Reactivity of Alkoxide and Hydroxide Complexes of Rhodium(I) and Iridium(I). *Organometallics* **1989**, *8*, 659–666. [[CrossRef](#)]
126. Makote, R.; Collinson, M.M. Template Recognition in Inorganic–Organic Hybrid Films Prepared by the Sol–Gel Process. *Chem. Mater.* **1998**, *10*, 2440–2445. [[CrossRef](#)]
127. Luo, Q.; Nie, F.; Long, X.; Qiao, Z.; Yang, G.; Ma, Y. Preparation of Nano-Fe<sub>2</sub>O<sub>3</sub> by CO<sub>2</sub>-Supercritical-Process-Assisted Sol-Gel Method. *Curr. Nanosci.* **2014**, *10*, 722–729. [[CrossRef](#)]
128. Guan, H.; Ke, Q.; Lv, C.; Zeng, N.; Hu, C.; Wang, S.; Ge, X.; Cai, J. Amorphous Iridium Oxide Nanoparticle Films Prepared by Low-Temperature Annealing and Plasma Treatment as Highly Efficient Oxygen Evolution Electrocatalysts. *Chem. Lett.* **2020**, *49*, 705–708. [[CrossRef](#)]
129. Yagi, M.; Tomita, E.; Sakita, S.; Kuwabara, T.; Nagai, K. Self-Assembly of Active IrO<sub>2</sub> Colloid Catalyst on an ITO Electrode for Efficient Electrochemical Water Oxidation. *J. Phys. Chem. B* **2005**, *109*, 21489–21491. [[CrossRef](#)] [[PubMed](#)]
130. Zu, L.; Qian, X.; Zhao, S.; Liang, Q.; Chen, Y.E.; Liu, M.; Su, B.-J.; Wu, K.-H.; Qu, L.; Duan, L.; et al. Self-Assembly of Ir-Based Nanosheets with Ordered Interlayer Space for Enhanced Electrocatalytic Water Oxidation. *J. Am. Chem. Soc.* **2022**, *144*, 2208–2217. [[CrossRef](#)]
131. Jiang, Y.; Fang, Y.; Chen, C.; Ni, P.; Kong, B.; Song, Z.; Lu, Y.; Niu, L. Amorphous Cobalt Boride Nanosheets Directly Grown on Nickel Foam: Controllable Alternately Dipping Deposition for Efficient Oxygen Evolution. *ChemElectroChem* **2019**, *6*, 3684–3689. [[CrossRef](#)]
132. Lee, J.; Kim, I.; Park, S. Boosting Stability and Activity of Oxygen Evolution Catalyst in Acidic Medium: Bimetallic Ir–Fe Oxides on Reduced Graphene Oxide Prepared through Ultrasonic Spray Pyrolysis. *ChemCatChem* **2019**, *11*, 2615–2623. [[CrossRef](#)]
133. Mahmoud, S.A.; Al-Shomar, S.M.; Akl, A.A. Electrical Characteristics and Nanocrystalline Formation of Sprayed Iridium Oxide Thin Films. *Adv. Condens. Matter Phys.* **2010**, *2010*, 518209. [[CrossRef](#)]

134. Park, N.-Y.; Kim, M.; Kim, Y.-H.; Ramesh, R.; Nandi, D.K.; Tsugawa, T.; Shigetomi, T.; Suzuki, K.; Harada, R.; Kim, M.; et al. Atomic Layer Deposition of Iridium Using a Tricarbonyl Cyclopropenyl Precursor and Oxygen. *Chem. Mater.* **2022**, *34*, 1533–1543. [[CrossRef](#)]
135. Cloward, I.N.; Liu, T.; Rose, J.; Jurado, T.; Bonn, A.G.; Chambers, M.B.; Pitman, C.L.; Ter Horst, M.A.; Miller, A.J.M. Catalyst Self-Assembly Accelerates Bimetallic Light-Driven Electrocatalytic H<sub>2</sub> Evolution in Water. *Nat. Chem.* **2024**, *16*, 709–716. [[CrossRef](#)] [[PubMed](#)]

**Disclaimer/Publisher's Note:** The statements, opinions and data contained in all publications are solely those of the individual author(s) and contributor(s) and not of MDPI and/or the editor(s). MDPI and/or the editor(s) disclaim responsibility for any injury to people or property resulting from any ideas, methods, instructions or products referred to in the content.